cells, Nrf2 dissociates from Keap1 following exposure to electrophiles, such that Nrf2 enters the nucleus in a more stable form. Our study has highlighted the rapid degradation of Nrf2 occurring in the cytosol compared to the slower degradation in the nucleus.

Discussion

In this study, we investigated the mechanism which underlies activation of the transcription factor Nrf2 by electrophiles leading to the expression of cellular defence genes against xenobiotic and oxidative insults. The present study demonstrated that nuclear accumulation of Nrf2 is an indispensable step for and strictly coincides with the induction of cellular defence genes. We also found that, in mouse peritoneal macrophages, the nuclear accumulation of Nrf2 requires Nrf2 protein to be newly synthesized.

Our current hypothesis for the accumulation of Nrf2 by electrophiles is depicted in Fig. 7. Whereas Nrf2 is rapidly turned over by the proteasome protein degradation system, electrophiles attenuate the degradation process by weakening the Nrf2–Keap1 interaction. Two lines of evidence support this contention. Firstly, the Nrf2-LacZ fusion gene knock-in mouse analysis provides convincing evidence that the N-terminal portion of Nrf2 is essential for the accumulation of Nrf2 in response to electrophiles *in vivo*. Secondly, Nrf2 is accumulated constitutively in the nuclei of *keap1*$^{-/-}$ macrophages at a level that did not increase further in response to electrophiles. We surmise that, in the absence of Keap1, Nrf2 protein escapes from the rapid cytosolic degradation process and becomes relatively stabilized in the nuclei of *keap1*$^{-/-}$ cells. Thus, electrophiles stabilize Nrf2 by repressing the effect of Keap1 on Nrf2.

The results of this study support our contention that the accumulation of Nrf2 mainly occurs by exploiting a post-transcriptional mechanism. In fact, Nrf2 accumulation does not accompany an increase in Nrf2 mRNA. On the contrary, our previous analyses showed that transcription of the *nrf2* gene is induced by electrophiles, both in PE keratinocytes and *in vivo* (Kwak *et al.* 2001, 2002). Thus, the accumulation of Nrf2 can be achieved via multiple pathways, including transcriptional and post-transcriptional mechanisms.

Amongst the possible post-transcriptional mechanisms, it appears that Nrf2 accumulates through the stabilization of Nrf2 protein in peritoneal macrophages. Two lines of evidence are noteworthy here. First, in addition to proteasome inhibitors, electrophiles markedly prolonged the degradation half-life of Nrf2. Second, electrophiles, such as DEM, and proteasome inhibitors, did not show any additive effect on the accumulation of Nrf2 (Fig. 3D). These results support our assertion that electrophiles act as inducers through the stabilization of Nrf2 protein by displacing it from proteasome-mediated degradation.

The down-regulation of key regulatory proteins is essential in many biological processes, including cell cycle control and signal transduction. In such processes, the down-regulation is often brought about by specific proteolysis mediated by the ubiquitin-proteasome system

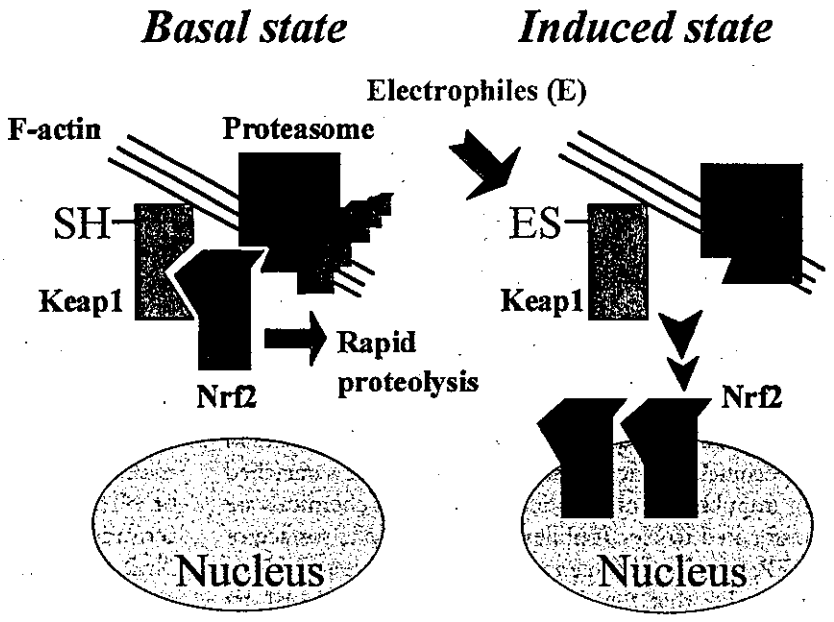

Figure 7 Hypothesis of Nrf2 activation. Keap1 and proteasome co-localize in the actin cytoskeleton. Keap1 localizes Nrf2 in the vicinity of the proteasome, thereby enhancing its degradation in the cytoplasm of quiescent cells. Sulfhydril reagents interact with the reactive cysteine(s) of Keap1, thus liberating Nrf2 from Keap1 repression. The dissociation of Nrf2 from Keap1 leads to the nuclear localization of Nrf2 with concomitant stabilization.

(Hochstrasser 1996; Varshavsky 1997). Alternatively, specific inhibitory proteins are known to bind and inhibit important regulatory proteins. One prominent example for the latter mechanism is the NF-κB/IκB system, in which IκB binds to NF-κB and sequesters it stably in the cytoplasm in the absence of inducing signals. Since Nrf2 is activated by electrophiles through its dissociation from Keap1 (Itoh *et al.* 1999a,b), Jaiswal and colleagues recently proposed that an analogous activation mechanism exists between Nrf2 and NF-κB (Dhakshinamoorthy & Jaiswal 2001). However, the finding that Nrf2 is rapidly degraded by proteasomes argues against such a claim. The Nrf2 activation mechanism rather shares a common feature with the hypoxia inducible transcription factors, hypoxia inducible factor-1α (HIF-1α) and HLF (HIF-1-like factor or EPAS-1). HIF-1α and HLF are rapidly degraded by proteasomes during normoxia through the hydroxylation of specific proline and/or aspartate residues, but stabilized under conditions of hypoxia (reviewed in Semenza 2001). However, the rapid turnover of Nrf2 is prevented by electrophiles through dissociation from Keap1, and this mechanism is completely different from that of the hypoxia inducible transcription factors. Thus, these results demonstrate that the activation mechanism of Nrf2 is a unique biological system.

Both *keap1* gene ablation and DEM result in the freedom of Nrf2 to translocate to the nucleus and accumulate, and these events appear to play an important role in the stabilization of Nrf2. It is becoming evident that the fast and efficient proteolysis of a short-lived protein not only depends on the presence of a degradation signal, but also requires a specific localization of the substrate (Lenk & Sommer 2000). This most probably reflects the fact that components of the ubiquitin proteasome system are not evenly distributed throughout the cell, but localize specifically to certain subcellular compartments (Hirsch & Ploegh 2000). Endoplasmic reticulum-associated protein degradation (ERAD) provides a prime example of compartmentalization of the ubiquitin proteasome system (Sommer & Wolf 1997). ERAD components localize on the cytosolic surface of the ER membrane and are responsible for the degradation, not only of misfolded proteins in the ER lumen, but of cytosolic proteins such as the transcriptional repressor Matα2 (Swanson *et al.* 2001).

Keap1 binds to the actin cytoskeleton and localizes in the perinuclear space where the ER network is enriched (our unpublished observation). Since most chemicals are transformed to electrophiles on the cytosolic surface of the ER membrane (Guengerich 1990), it is reasonable to hypothesize that the direct modification of Keap1 by reactive electrophiles takes place near the cytosolic surface of the ER membrane. Similarly, as the 20S proteasome is located at the cytoskeleton of intermediate and actin filaments (Arcangeletti *et al.* 2000), an alternative possibility is that Keap1 mediated sequestration of Nrf2 to the actin cytoskeleton might be essential for rapid Nrf2 degradation (Figs 6C and 7). Since Nrf2 protein in the nucleus is still sensitive to proteasomal degradation in *keap1*$^{-/-}$ cells (Fig. 6A), the Nrf2 degradation activity, albeit weaker, must also exist in the nucleus as well as in the cytosol. In the nucleus, considering the absence of Keap1, it is unlikely that Keap1 is directly involved in the recognition of Nrf2 by proteasome. In the case of the cytoplasm, however, Keap1 is likely to determine the localization of Nrf2 to the proteasome, thereby enhancing Nrf2 degradation.

We demonstrated, by its linkage to EGFP, that the Neh2 domain is responsible for Nrf2 degradation, at least in part. The Neh2 domain can be divided into three subdomains based on interspecies amino acid conservation. These subdomains comprise an N-terminal amphipathic helix subdomain, which is conserved in Nrf1 and nematode SKN-1 (Itoh *et al.* 1999b), a central hydrophilic region, and a Keap1 binding ETGE motif at the C-terminus (Itoh *et al.* 1999b; Kobayashi *et al.* 2002). It is interesting to note that the hydrophobic surface of the amphipathic helix present in the Matα2 N-terminal region is the major structural feature of the Matα2 degradation signal (Johnson *et al.* 1998). The Ubc6p-Ubc7p ubiquitin-conjugating enzyme pair, which is a component of ERAD, mediates this type of degradation signal (Gilon *et al.* 2000; Sadis *et al.* 1995). Thus, the hydrophobic surface of the Neh2 amphipathic helix might be important for Nrf2 degradation.

Quite recently, it was reported that Nrf2 is degraded through the ubiquitin–proteasome pathway, and that phase II inducers stabilize Nrf2 against degradation (Nguyen *et al.* 2002; Sekhar *et al.* 2002; Stewart *et al.* 2002). The mechanisms as to how Nrf2 is stabilized, however, remain to be clarified. Furthermore, it should be tested carefully through *in vivo* systems whether recognition of Nrf2 by the proteasome system requires ubiquitination and whether such Nrf2 ubiquitination is regulated by electrophiles. Interestingly, Nrf2 is stabilized by cadmium without any apparent changes in ubiquitination status (Stewart *et al.* 2002), suggesting that any changes in Nrf2 ubiquitination may not be associated with its stabilization. On the contrary, phosphorylation of Nrf2 has been shown to be important for Nrf2 activation (Huang *et al.* 2002) and it was reported that Nrf2 stabilization by tert-butylhydroquinone (tBHQ) was inhibited by MAP kinase inhibitors, but not by

protein kinase C (PKC) inhibitors (Nguyen *et al.* 2002). Thus, the MAPK pathway may be responsible for the tBHQ-mediated accumulation of Nrf2, although future studies will be absolutely essential for shedding light on the relationship between the function of Keap1 and the modification of Nrf2 by the kinase pathways or ubiquitination pathway in the Nrf2 degradation process.

The rapid cytosolic degradation of Nrf2 seems to have a physiological relevance. When the cell encounters highly toxic electrophiles, a state of emergency arises in which it is vital that potent transactivators such as Nrf2 (Katoh *et al.* 2001) can rapidly and effectively provide cytoprotection. One drawback is that potent transcriptional activators may place cells under the possible danger of deregulated activation. Indeed, mice with constitutively activated Nrf2 due to the absence of Keap1 die within 3 weeks of birth, most probably due to excessive Nrf2 mediated transcription (manuscript submitted for publication). The rapid and irreversible proteolysis of Nrf2 in the cytosol might provide a solid basis for the tight control of Nrf2 activity.

One question remaining is whether the stabilization *per se* triggers Nrf2 activation or not. Since Nrf2 overexpression can cause the constitutive expression of an ARE reporter gene in cell culture (Itoh *et al.* 1999a) and an endogenous Nrf2 target gene *in vivo* (Kobayashi *et al.* 2002), it is plausible that the saturation of Keap1 repression can lead to Nrf2 activation. Proteasome inhibition can result in the accumulation of Nrf2 in the nucleus (Fig. 3A) and the subsequent induction of target gene expression (our unpublished observations; Sekhar *et al.* 2000); thus, protein stabilization might at least enhance the nuclear translocation of Nrf2 in response to inducers (Fig. 7). Further analysis, however, is required to elucidate the degradation mechanisms of Nrf2.

Experimental procedures

Plasmid construction

Construction of the Neh2-EGFP expression plasmid was previously described (Kobayashi *et al.* 2002). To generate the Neh5-EGFP expression plasmid, a cDNA fragment encoding the Neh5 region (amino acids 153–227) of Nrf2 was amplified by PCR and subcloned into the *KpnI* and *AgeI* sites of pcDNA3-EGFP (Kobayashi *et al.* 2002).

Cell culture and treatment

Mouse peritoneal macrophages were cultured as previously described (Ishii *et al.* 2000). Cells were treated with 10 μM MG132 (Peptide Institute Inc.), 50 μM MG115 (Peptide Institute Inc.), 10 μM clasto-Lactacystin β-Lactone (Calbiochem), or 10 μM calpain inhibitor (Peptide Institute Inc.). The cells were also treated with 2.5 μM menadione, 100 μM DEM, 10 μM 1-chloro-2-4-dinitrobenzene (CDNB) or 10 μM sulforaphane. To remove the MG132 from the culture, the cells were washed three times with medium, with incubations of 5 min each. NIH 3T3 fibroblast cells were maintained in DMEM supplemented with 10% FBS and stable clones were selected in the presence of 0.5 mg/mL G418.

Immunoblotting

Total cell extracts or fractionated extracts were separated by SDS–polyacrylamide gel electrophoresis in the presence of 2-mercaptoethanol and electro-transferred on to Immobilon membrane (Millipore, Bedford, MA). The membrane was blocked in 3% skimmed milk and 2% goat serum overnight at 4 °C and subsequently incubated with anti-Nrf2 antibody (Ishii *et al.* 2000) overnight at 4 °C. As a loading control, the membrane was also hybridized with anti-β-actin antibody or anti-lamin B antibody. To detect immunoreactive proteins, we used horseradish peroxidase-conjugated anti-rabbit IgG and ECL blotting reagents (Amersham Japan, Tokyo).

RNA blot analysis

Total cellular RNA was extracted from macrophages by RNAzol™ B (Tel-Test Inc., Friendswood, TX). The RNA samples (10 μg) were electrophoresed and transferred on to Zeta-Probe GT membranes (Bio-Rad Japan, Tokyo). The membranes were probed with [^{32}P]-labelled cDNA probes, as indicated in the figures. β-Actin cDNA was used as a positive control.

Cell fractionation

Nuclear extracts from macrophages were prepared as previously described (Ishii *et al.* 2000). Briefly, 7.5×10^6 peritoneal macrophages were suspended in hypotonic buffer and vortexed for 15 s and the nuclear fraction was pelleted at 7700 *g* for 1 min. The nuclei were resuspended in SDS sample loading buffer (without dye or 2-mercaptoethanol) and boiled for 5 min. Protein concentrations were estimated by BCA protein assay (Pierce, Rockford, IL). 0.5% Triton X soluble and insoluble fractions were prepared as previously described (Fey *et al.* 1984).

Immunohistochemistry

Livers or intestines were fixed in ice-cold 10% formalin in phosphate-buffered saline for 2 h, dehydrated with ethanol, embedded in paraffin, and cut into 3 μm sections. The sections were de-waxed and incubated for 20 min with anti-β-galactosidase antibody. They were then incubated with biotin-conjugated goat anti-rabbit IgG and avidin-DAB.

Acknowledgements

We are grateful to Drs Thomas Kensler, Mi-Kyoung Kwak, Satoru Takahashi and Kazuhiko Igarashi for critical discussions and

advice. We also thank Ms N. Kaneko for technical support in histological analysis and R. Kawai for mouse breeding. This work was supported by grants from the Japan Science and Technology Corporation-ERATO project (M.Y.), Ministry of Education, Culture, Sports, Science and Technology of Japan (K.I., I.T. and M.Y.), Japanese Society for Promotion of Sciences (JSPS)-RFTF (M.Y.), and Probrain (K.I.). N.W. was a JSPS postdoctoral fellow.

References

Alam, J., Camhi, S. & Choi, A.M. (1995) Identification of a second region upstream of the mouse heme oxygenase-1 gene that functions as a basal level and inducer-dependent transcriptional enhancer. *J. Biol. Chem.* **270**, 11977–11984.

Aoki, Y., Sato, H., Nishimura, N., Takahashi, S., Itoh, K. & Yamamoto, M. (2001) Accelerated DNA adduct formation in the lung of the Nrf2 knockout mouse exposed to diesel exhaust. *Toxicol. Appl. Pharmacol.* **173**, 154–160.

Arcangeletti, C., De Conto, F., Sutterlin, R., *et al.* (2000) Specific types of prosomes distribute differentially between intermediate and actin filaments in epithelial, fibroblastic and muscle cells. *Eur. J. Cell Biol.* **79**, 423–437.

Beutler, T.M., Gallagher, E.P., Wang, C., Stahl, D.L., Hayes, J.D. & Eaton, D.L. (1995) Induction of phase I and phase II drug metabolizing enzyme mRNA, protein and activity by BHA, ethoxyquin and oltipraz. *Toxicol. Appl. Pharmacol.* **135**, 45–57.

Dhakshinamoorthy, S. & Jaiswal, A.K. (2001) Functional characterization and role of INrf2 in antioxidant response element-mediated expression and antioxidant induction of NAD(P)H: quinone oxidoreductase1 gene. *Oncogene* **20**, 3906–3917.

Enomoto, A., Itoh, K., Nagayoshi, E., *et al.* (2001) High sensitivity of Nrf2 knockout mice to acetaminophen hepatotoxicity associated with decreased expression of ARE-regulated drug metabolizing enzymes and antioxidant genes. *Toxicol. Sci.* **59**, 169–177.

Fey, E.G., Wan, K.M. & Penman, S. (1984) Epithelial cytoskeletal framework and nuclear matrix intermediated filament scaffold: three-dimensional organization and protein composition. *J. Cell Biol.* **98**, 1973–1984.

Friling, R.S., Bensimon, S. & Daniel, V. (1990) Xenobiotic-inducible expression of murine glutathione S-transferase Ya subunit gene is controlled by an electrophile-responsive element. *Proc. Natl. Acad. Sci. USA* **87**, 6258–6262.

Gilon, T., Chomsky, O. & Kulka, R.G. (2000) Degradation signals recognized by the Ubc6p-Ubc7p ubiquitin-conjugating enzyme pair. *Mol. Cell. Biol.* **20**, 7214–7219.

Guengerich, F.P. (1990) Enzymatic oxidation of xenobiotic chemicals. *Crit. Rev. Biochem. Mol. Biol.* **25**, 97–153.

Hayes, J.D. & Pulford, J.D. (1995) The glutathione S-transferase supergene family: Regulation of GST and the contribution of the isozymes to cancer chemoprevention and drug resistance. *Crit. Rev. Biochem. Mol. Biol.* **30**, 445–600.

Hirsch, C. & Ploegh, H.L. (2000) Intracellular targeting of the proteasome. *Trends Cell Biol.* **10**, 268–272.

Hochstrasser, M. (1996) Ubiquitin-dependent protein degradation. *Annu. Rev. Genet.* **30**, 405–439.

Huang, H.C., Nguyen, T. & Pickett, C.B. (2002) Phosphorylation of Nrf2 at Ser-40 by protein kinase C regulates antioxidant response element-mediated transcription. *J. Biol. Chem.* **277**, 42769–42774.

Ishii, T., Itoh, K., Takahashi, S., *et al.* (2000) Transcription factor Nrf2 coordinately regulates a group of oxidative stress-inducible genes in macrophages. *J. Biol. Chem.* **275**, 16023–16029.

Ishii, T., Itoh, K. & Yamamoto, M. (2002) Roles of Nrf2 in activation of antioxidant enzyme genes via antioxidant responsive elements. *Meth. Enzymol.* **348**, 182–190.

Itoh, K., Chiba, T., Takahashi, S., *et al.* (1997) An Nrf2/small maf heterodimer mediates the induction of phase II detoxifying enzyme genes through antioxidant responsive element. *Biochem. Biophys. Res. Commun.* **236**, 313–322.

Itoh, K., Igarashi, K., Hayashi, N., Nishizawa, M. & Yamamoto, M. (1995) Cloning and characterization of a novel erythroid cell-derived CNC family transcription factor heterodimerizing with the small maf family proteins. *Mol. Cell. Biol.* **15**, 4184–4193.

Itoh, K., Ishii, T., Wakabayashi, N. & Yamamoto, M. (1999b) Regulatory mechanisms of cellular response to oxidative stress. *Free Radic. Res.* **31**, 319–324.

Itoh, K., Wakabayashi, N., Katoh, Y., *et al.* (1999a) Keap1 represses nuclear activation of antioxidant responsive elements by Nrf2 through binding to the amino-terminal Neh2 domain. *Genes Dev.* **13**, 76–86.

Johnson, P.R., Swanson, R., Rakhilina, L. & Hochstrasser, M. (1998) Degradation signal masking by heterodimerization of MATalphα2 and MATα1 blocks their mutual destruction by the ubiquitin-proteasome pathway. *Cell* **94**, 217–227.

Katoh, Y., Itoh, K., Yoshida, E., Miyagishi, M., Fukamizu, A. & Yamamoto, M. (2001) Two domains of Nrf2 cooperatively bind CBP, a CREB binding protein, and synergistically activate transcription. *Genes Cells* **6**, 857–868.

Kim, Y.C., Masutani, H., Yamaguchi, Y., Itoh, K., Yamamoto, M. & Yodoi, J. (2001) Hemin-induced activation of the thioredoxin gene by Nrf2. A differential regulation of the antioxidant responsive element by a switch of its binding factors. *J. Biol. Chem.* **276**, 18399–18406.

Kobayashi, M., Itoh, K., Suzuki, T., *et al.* (2002) Identification of the interactive interface and phylogenic conservation of the Nrf2-Keap1system. *Genes Cells* **7**, 807–820.

Kwak, M.K., Itoh, K., Yamamoto, M. & Kensler, T.W. (2002) Enhanced expression of the transcription factor Nrf2 by cancer chemopreventive agents: role of antioxidant response element-like sequences in the nrf2 promoter. *Mol. Cell. Biol.* **22**, 2883–2892.

Kwak, M.K., Itoh, K., Yamamoto, M., Sutter, T.R. & Kensler, T.W. (2001) Role of transcription factor Nrf2 in the induction of hepatic phase 2 and antioxidative enzymes in vivo by the cancer chemoprotective agent, 3H-1, 2-dimethiole-3-thione. *Mol. Med.* **7**, 135–145.

Lee, D.H. & Goldberg, A.L. (1998) Proteasome inhibitors: valuable new tools for cell biologists. *Trends Cell Biol.* **8**, 397–403.

Lenk, U. & Sommer, T. (2000) Ubiquitin-mediated proteolysis of a short-lived regulatory protein depends on its cellular localization. *J. Biol. Chem.* **275**, 39403–139410.

Marini, M.G., Chan, K., Casula, L., Kan, Y.W., Cao, A. & Moi, P. (1997) hMAF, a small human transcription factor that heterodimerizes specifically with Nrf1 and Nrf2. *J. Biol. Chem.* **272**, 16490–16497.

Moi, P., Chan, K., Asunis, I., Cao, A. & Kan, Y.W. (1994) Isolation of NF-E2-related factor 2 (Nrf2), a NF-E2-like basic leucine zipper transcriptional activator that binds to the tandem NF-E2/AP1 repeat of the beta-globin locus control region. *Proc. Natl. Acad. Sci. USA* **91**, 9926–9930.

Motohashi, H., Shavit, J.A., Igarashi, K., Yamamoto, M. & Engel, J.D. (1997) The world according to Maf. *Nucl. Acids Res.* **25**, 2953–2959.

Mulcahy, R.T., Wartman, M.A., Bailey, H.H. & Gipp, J.J. (1997) Constitutive and β-naphthoflavone-induced expression of the human γ-glutamylcysteine synthetase heavy subunit gene is regulated by a distal antioxidant response element/TRE sequence. *J. Biol. Chem.* **272**, 7445–7454.

Nguyen, T., Sherratt, P.J., Huang, H.C., Yang, C.S. & Pickett, C.B. (2003) Increased protein stability as a mechanism that enhances Nrf2-mediated transcriptional activation of the antioxidant response element: degradation of Nrf2 by the 26S proteasome. *J. Biol. Chem.* **278**, 4536–4541.

Prestera, T., Zhang, Y., Spencer, R.S., Wilczak, A.C. & Talalay, P. (1993) The electrophile counterattack response: protection against neoplasia and toxicity. *Adv. Enzyme Regul.* **33**, 281–296.

Primiano, T., Sutter, T.R. & Kensler, T.W. (1997) Antioxidant-inducible genes. *Adv. Pharmacol.* **38**, 293–328.

Ramos-Gomez, M., Kwak, M.K., Dolan, P.M., *et al.* (2001) Sensitivity to carcinogenesis is increased and chemoprotective efficacy of enzyme inducers is lost in nrf2 transcription factor-deficient mice. *Proc. Natl. Acad. Sci. USA* **98**, 3410–3415.

Rushmore, T.H., Morton, M.R. & Pickett, C.B. (1991) The antioxidant responsive element. *J. Biol. Chem.* **266**, 11632–11639.

Sadis, S., Atienza, C. Jr & Finley, D. (1995) Synthetic signals for ubiquitin-dependent proteolysis. *Mol. Cell. Biol.* **15**, 4086–4094.

Sekhar, K.R., Soltaninassab, S.R., Borrelli, M.J., *et al.* (2000) Inhibition of the 26S proteasome induces expression of GLCLC, the catalytic subunit for gamma-glutamylcysteine synthetase. *Biochem. Biophys. Res. Commun.* **270**, 311–317.

Sekhar, K.R., Yan, X.X. & Freeman, M.L. (2002) Nrf2 degradation by the ubiquitin proteasome pathway is inhibited by KIAA0132, the human homolog to INrf2. *Oncogene* **21**, 6829–6834.

Semenza, G.L. (2001) HIF-1, O (2), and the 3 PHDs: how animal cells signal hypoxia to the nucleus. *Cell* **107**, 1–3.

Sommer, T. & Wolf, D.H. (1997) Endoplasmic reticulum degradation: reverse protein flow of no return. *FASEB J.* **11**, 1227–1233.

Stewart, D., Killeen, E., Naquin, R., Alam, S. & Alam, J. (2003) Degradation of transcription factor Nrf2 via the ubiquitin-proteasome pathway and stabilization by cadmium. *J. Biol. Chem.* **278**, 2396–2402.

Swanson, R., Locher, M. & Hochstrasser, M. (2001) A conserved ubiquitin ligase of the nuclear envelope/endoplasmic reticulum that functions in both ER-associated and Matα2 repressor degradation. *Genes Dev.* **15**, 2660–2674.

Varshavsky, A. (1997) The ubiquitin system. *Trends Biochem. Sci.* **22**, 383–387.

Received: 5 December 2002
Accepted: 15 January 2003

Free Radical Biology & Medicine, Vol. 34, No. 10, pp. 1236–1242, 2003

0891-5849/03/$–see front matter

ELSEVIER

doi:10.1016/S0891-5849(03)00073-X

Original Contribution

EPR IMAGING OF REDUCING ACTIVITY IN Nrf2 TRANSCRIPTIONAL FACTOR-DEFICIENT MICE

AKI HIRAYAMA,* KEIGYOU YOH,* SOHJI NAGASE,* ATSUSHI UEDA,* KEN ITOH,†‡ NAOKI MORITO,*† KOUICHI HIRAYAMA,* SATORU TAKAHASHI,† MASAYUKI YAMAMOTO,†‡ and AKIO KOYAMA*

*Institute of Clinical Medicine, †Institute of Basic Medical Sciences; and ‡Center for Tsukuba Advanced Research Alliance, University of Tsukuba, Ibaraki, Japan

(*Received* 29 *August* 2002; *Revised* 23 *December* 2002; *Accepted* 30 *January* 2003)

Abstract—Mice that lack the Nrf2 (NF-E2-related factor 2) transcription factor develop a lupus-like autoimmune nephritis. The tissue-reducing activity of Nrf2-deficient mice was evaluated using a combination of real-time EPR imaging and spin probe kinetic analysis. Substantial delay in the spin probe 3-carbamoyl-2,2,5,5-tetramethylpyrrolidine-1-oxyl (Carbamoyl-PROXYL) disappearance in the liver and kidneys of Nrf2-deficient mice was observed by EPR imaging. The half-life of the spin probe in the upper abdominal area was prolonged in both the Nrf2-deficient mice and in aged mice. The combination of Nrf2 deficiency and aging in female mice resulted in the most prolonged half-life of disappearance, which was four times longer than that of juvenile female mice with a wild-type genotype. These results indicate that the low reducing activity in these organs is brought about by both Nrf2 deficiency and the aging process, and it may play a key role in the onset of autoimmune nephritis. This combination of the EPR imaging and half-life analysis appears to be a very powerful tool in the real-time analysis of reducing activity.

Keywords—EPR, EPR imaging, Nrf2, Carbamoyl-PROXYL, Lupus nephritis, Free radicals

INTRODUCTION

As the pathophysiological role of reactive oxygen species (ROS) in many diseases becomes clear, the importance of analyzing in vivo ROS kinetics increases. While there is a pressing need for direct measurement of both oxidative stress and antioxidant status in vivo, free radicals, because of their short half-lives, are often estimated indirectly by their end products or gene-related products. Electron paramagnetic resonance (EPR), which is a technique for the detection of intramolecular unpaired electrons, meets the need for direct measurement of free radicals. Although the conventional X-band EPR system is not suitable for in vivo work because of water-induced dielectric loss, the recent development of low frequency EPR (L-band EPR) has circumvented this problem and in vivo EPR measurement is now possible [1]. In this study we have applied a newly developed in vivo three-dimensional (3D) stereoscopic EPR imaging system for the analysis of the organ-reducing activity of a wild-type and a germ line Nrf2 (NF-E2-related factor 2) mutant mouse [2]. The Nrf2 mutant mouse shows an increased level of oxidative stress, which may bear some relation to the onset of disease.

Nrf2 is a basic leucine zipper-type transcriptional activator essential for the coordinate transcriptional induction of antioxidant enzymes and phase II drug-metabolizing enzymes through interaction with antioxidant-responsive element/electrophile-responsive element (ARE/EpRE). AREs are usually found in the regulatory sequences of antioxidant enzyme genes, such as heme oxygenase-1 (HO-1) [3] and γ-glutamylcysteine synthetase [4], and regulate a wide range of metabolic responses provoked by ROS or electrophiles [5]. In consequence of these abnormalities, Nrf2-deficient female mice are very sensitive to oxidative stress [6], generate increased amounts of lipid peroxidative products, and have a shorter life span compared to their wild-type counterparts [7]. Additionally, these mice develop a severe lupus-like glomerulonephritis [7]. Thus, Nrf2-deficient female mouse is a new model of lupus-like auto-

Address correspondence to: Dr. Aki Hirayama, University of Tsukuba, Institute of Clinical Medicine, Department of Internal Medicine, 1-1-1 Tennoudai, Tsukuba-City, Ibaraki 305-8547, Japan; Tel: +81 298-533202; Fax: +81 298-533202; E-Mail: aki-hira@md.tsukuba.ac.jp.

immune nephritis, which is closely related to increased oxidative stress.

Using a noninvasive in vivo EPR system, we have evaluated the organ-reducing activity of the mice at young (10 weeks old) and elderly (50 weeks old) stages. An important characteristic of the Nrf2-deficient mouse is the slow onset of glomerulonephritis. The first detection of a glomerular lesion in an Nrf2-deficient female mouse is at around 40 weeks, and significant glomerular damage is found after 60 weeks of age [7]. This onset of nephritis is much later than occurrences in other lupus mouse models such as MRL/*lpr* and NZB/W [8,9]. Consequently, we believe that not only genetic features but also the redox status play important roles in the progression of this glomerulonephritis. Thus, the noninvasive analysis of redox status is an important parameter in this study.

In this study, we analyzed organ-reducing activity of Nrf2-deficient mice using (i) 3D-stereoscopic EPR imaging, (ii) rate constants of the reaction for the spin probe disappearance, and (iii) ex vivo measurement system of total reducing activity in various organ homogenates. For the EPR spin probe, 3-carbamoyl-2,2,5,5-tetramethylpyrrolidine-1-oxyl (Carbamoyl-PROXYL) was used.

MATERIALS AND METHODS

Animals

The generation of Nrf2-deficient mice has been described [2]. The mice used in this study were of ICR background. Female Nrf2-deficient mice aged around 10 weeks (juvenile) or 50 weeks (elderly) were used for this study (n = 4 and 5, respectively). Female wild-type mice of similar ages were employed for controls (n = 4 for juvenile and 5 for elderly). All experiments were performed according to the Guide for the Care and Use of Laboratory Animals in University of Tsukuba.

Imaging study

Carbamoyl-PROXYL (200 mM, 3 ml/kg) was injected into the animals through the tail vein 15 min after pentobarbital anesthesia. Each mouse was then fixed in a plastic holder and put in the EPR system placing its upper abdominal area in the center; the bladder was outside of the resonator. Three-dimensional (3D) EPR images were constructed with the center peak of the triplet Carbamoyl-PROXYL EPR signal using ESR-CT version 1.136 software (JEOL, Tokyo, Japan). EPR conditions were as follows: field gradient, 1.0 mT/cm; changing direction, 30° steps (provides six spectra for each projection); magnetic field, 37.0 ± 5.0 mT; microwave power, 0.25 mW; and, modulation width, 0.1 mT. Because there are no practical internal standard markers for L-band measurements, equivalence of the resonator conditions was confirmed with (i) the signal threshold value used for the image construction; and, (ii) the longitudinal size of a DPPH marker with each mouse, which were imaged prior to the Carbamoyl-PROXYL injection. The cross-sectional 3D EPR images were obtained every 5 min until 15 min after Carbamoyl-PROXYL injection. Stereoscopic images in 3D were constructed using 3D cross-sectional data with IRIS explorer software (IRIS Co., Berkshire, England).

In vivo ESR measurement of Carbamoyl-PROXYL signal disappearance

The signal intensity was measured using ESR-NT software (JEOL). Rate constants were measured every 60 s from 4 to 40 min after the Carbamoyl-PROXYL injection. The peak-to-peak height of the lowest magnetic field signal in the triplet spectrum was defined as the signal intensity. EPR conditions for these in vivo measurements were as follows: magnetic field, 37.0 ± 5.0 mT; modulation width, 0.69 mT; time constant, 0.03 s; microwave power, 0.25 mW; and, scanning time, 30 s. The spin clearance of the Carbamoyl-PROXYL signal intensity was semilogarithmically plotted against time. The first order spin reduction rate constant was estimated from the slope value of the observed clearance curve, which was obtained by best fit. The half-life was calculated using the equation: $t1/2 = \ln 2/k$.

Ex vivo measurements of organ-reducing activity

The mice were sacrificed immediately after the imaging study and the abdominal organs were removed. The remaining Carbamoyl-PROXYL quantities in the homogenates from these organs were measured using conventional X-band EPR equipment (TR-25, JEOL) and a quartz flat EPR cell (Labotec, Tokyo, Japan). Elapsed times from the Carbamoyl-PROXYL injection to sacrifice, to removal of the kidney and the liver, and to the X-band EPR examinations were fixed. Mice were sacrificed 16 min after the injection and the organs were removed within 1 min. These organs were homogenized on ice followed by X-band measurements. Renal and hepatic homogenates were measured 17 and 23 min, respectively, after the injection. The peak-to-peak height of the lowest magnetic field signal in the triplet spectrum was defined as the signal intensity of Carbamoyl-PROXYL. The ratio of intensities of Carbamoyl-PROXYL and a manganese oxide internal standard peak was defined as the remaining Carbamoyl-PROXYL signal intensity (Rem). After the measurements, the homogenates were combined with the same amount of 1.0 mM potassium ferricyanide. This process reoxidized EPR-silent hydroxylamines, which are already reduced by the

tissue, to EPR-positive Carbamoyl-PROXYL again. The signal intensity after the addition of potassium ferricyanide was defined as total tissue hydroxylamine (ReOx) [10]. The Rem/ReOx ratio was used as an index for tissue-reducing activity.

Statistical analysis

Significant differences between the groups of mice were analyzed by means of the unpaired Student's *t*-test; p values less than .05 were considered statistically significant. Results are expressed as means ± SD.

RESULTS

EPR imaging reveals a delay in the Carbamoyl-PROXYL disappearance in Nrf2-deficient mice

To analyze the in vivo redox status of the wild-type and Nrf2 mutant mice, age-matched wild types and Nrf2 germ line mutant mice were analyzed by in vivo 3D-stereoscopic EPR imaging. A typical three-line Carbamoyl-PROXYL signal was observed 3 min after the Carbamoyl-PROXYL injection (data not shown). EPR-positive regions were observed in the upper abdominal area of both aged wild-type mice and Nrf2-deficient mice 5 min after Carbamoyl-PROXYL injection. Typical 3D stereoscopic EPR images of aged mice from both wild types and Nrf2-deficient animals are shown in Figs. 1 and 2. Nrf2-deficient mice showed stronger and larger images corresponding to their hepatic and renal regions (Figs. 1b and 1d, pink color) than those seen in wild-type mice (Figs. 1a and 1c, green color). Tomographical analysis further supported this observation (Figs. 1e and 1f). In wild-type mice, images from the kidneys disappeared and the liver images were diminished 10 min after the Carbamoyl-PROXYL injection (Figs. 2a and 2b, green color). In contrast, the liver and kidney images of Nrf2-deficient mice were clearly visible at this time (Figs. 2c and 2d, pink color), indicating a decrease in reducing activity for the nitroxide radical in the Nrf2-deficient mice.

Fifteen minutes after the Carbamoyl-PROXYL injection, EPR signals were not detected in the wild-type mice. In contrast, weak EPR signals were observed in the Nrf2-deficient mice (data not shown). These results indicate that spin signals last longer in Nrf2-deficient mice than in wild types. Whereas the initial intensity of signals after Carbamoyl-PROXYL injection differs from mouse to mouse, the prolonged signal decay in Nrf2-deficient mice was quite reproducible.

Prolonged half-life of Carbamoyl-PROXYL in Nrf2-deficient mice

The reduction of Carbamoyl-PROXYL has been reported to follow first-order kinetics [11,12]. Showing good agreement with previous observations, the plots of signal intensities were fitted to straight lines on a semi-logarithmic scale with both the wild-type and Nrf2-deficient mice, indicating that Carbamoyl-PROXYL reduction obeyed first-order kinetics during the time measured (typical signal decay curves are shown in Fig. 3a). The half-time of Carbamoyl-PROXYL decay in the upper abdominal area was prolonged in the Nrf2-deficient mice (Fig. 3b). In elderly wild-type mice, the half-life of the probe was 27.2 ± 2.2 min ($n = 5$), which is significantly shorter than the half-life of elderly Nrf2-deficient mice at 54.0 ± 16.4 min ($n = 4$, $p < .05$, Fig. 3b). The half-life of Carbamoyl-PROXYL in juvenile mice was 12.1 ± 3.4 min ($n = 5$) and 20.0 ± 5.1 min ($n = 5$) for the wild-type and the Nrf2-deficient mice, respectively; this difference was statistically significant ($p < .05$). Both of these values were significantly lower than those in the corresponding elderly mice ($p < .01$). These results indicate that both aging and Nrf2 deficiency contribute to the low reducing activity in the organs examined.

Confirmation of decreased organ-reducing activity by ex vivo EPR analysis

Since EPR imaging detects paramagnetic substances only, each domain of the images reflects signal intensity in the area concerned rather than organ shape. Therefore, there still remains uncertainty in our assignment of the signals to the specific organs. To address whether these images truly correspond to the livers and kidneys, we sacrificed the animals and removed their abdominal organs. Livers and kidneys were homogenized and analyzed using conventional X-band EPR spectroscopy. The Rem/ReOx ratio was then used as an index of tissue-reducing activity (see Materials and Methods). This ex vivo study revealed higher Rem/ReOx ratios in the Nrf2-deficient mouse livers compared to the wild-type mouse livers ($p < .05$, Table 1). Increased Rem/ReOx ratio was also observed in the Nrf2-deficient mouse kidneys.

DISCUSSION

The disappearance of EPR signals from nitroxide spin probes is determined by two major factors: (i) a decrease in the tissue-reducing activity, which leads to prolongation of the signal disappearance; and, (ii) the reaction between spin probes and locally produced free radicals, which leads to accelerated EPR signal disappearance [13]. Nitroxide radicals including Carbamoyl-PROXYL

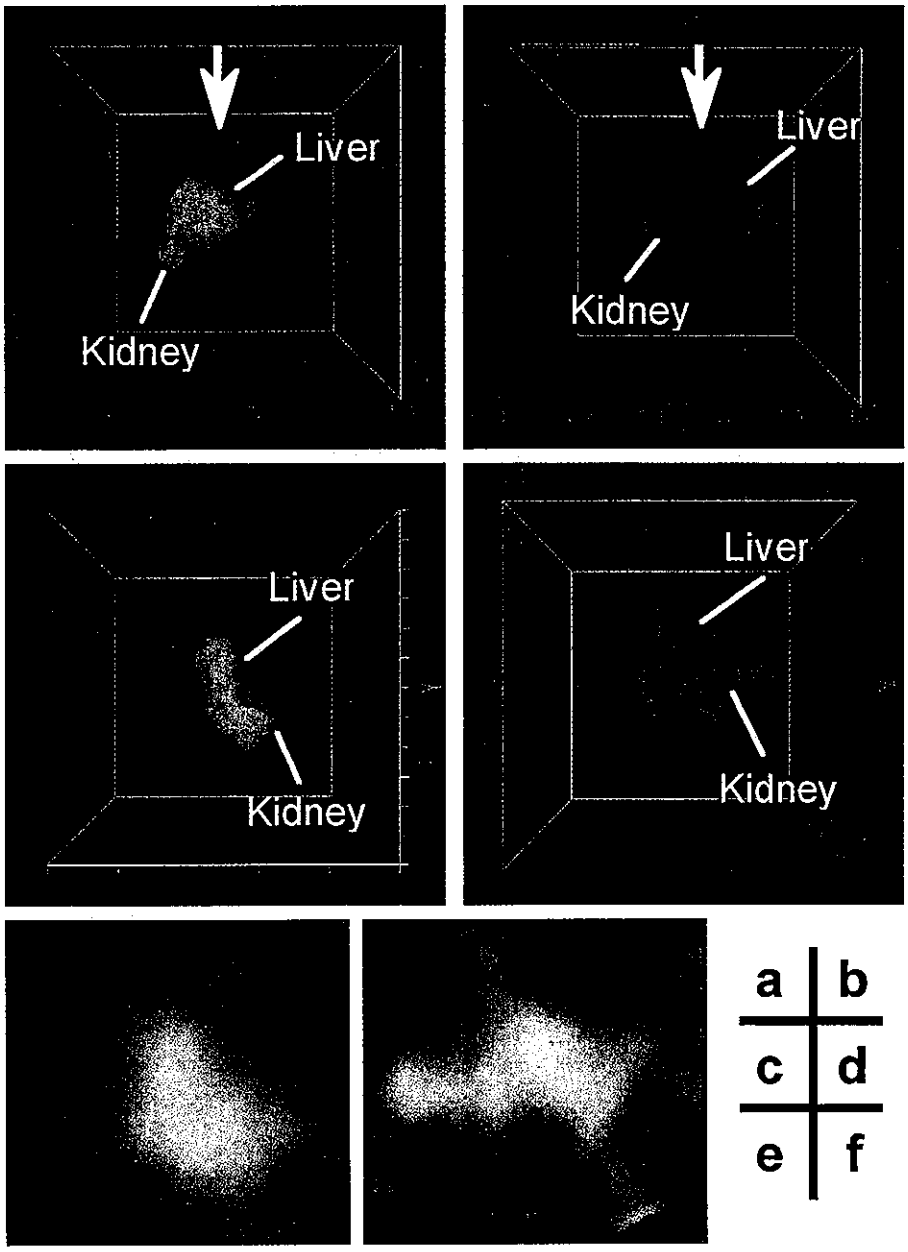

Fig. 1. Tomographical 3D stereoscopic images of aged wild-type and Nrf2-deficient mice 5 min after a Carbamoyl-PROXYL injection. Representative 3D stereoscopic EPR images of (a and b) lateral and (c and d) caudal views, and (e and f) caudal tomographical images from (a, c, and e) wild-type and (b, d, and f) Nrf2-deficient mice are shown. The arrows (a and b) indicate the positions of cross-sections that are shown on the (e and f) tomographical images. The image of both hepatic and renal areas remains strong in Nrf2-deficient mice. Carbamoyl-PROXYL (200 mM, 3 ml/kg) was injected into the mice through the tail vein under pentobarbital anesthesia. The mouse was fixed in the EPR system, placing its upper abdominal area in the center and the bladder outside of the resonator. The cross-sectional 3D EPR images were obtained every 5 min until 15 min after the Carbamoyl-PROXYL injection. EPR conditions were as follows: field gradient, 1.0 mT/cm; changing direction, 30° steps (provides six spectra for each projection); magnetic field, 37.0 ± 5.0 mT; microwave power, 0.25 mW; and, modulation width, 1.0 mT. Results are representative of three independent experiments.

are converted to the corresponding hydroxylamines with one-electron reductions that lead to a loss of the EPR signal [10,14]. Glutathione is known to play a central role in this paramagnetic loss among the various intracellular reductants, and one study showed correlations between glutathione levels and the Carbamoyl-PROXYL reduction rate constant [15]. The paramagnetic loss of the nitroxide radicals usually is not caused during reduction with components of blood, but rather after their transport to various organs [10]. Thus, altered tissue antioxidant activity in organs results in prolongation of the EPR signal decay. On the other hand, some nitroxide

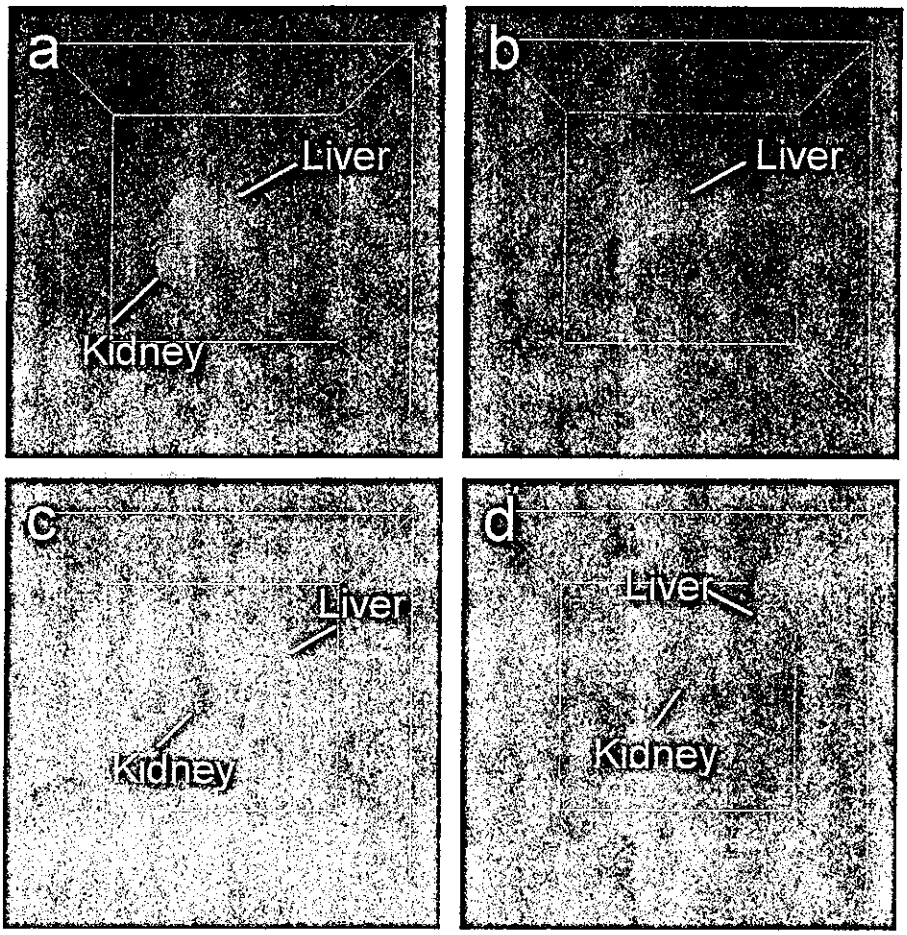

Fig. 2. Sequential changes in the lateral views of wild-type and Nrf2-deficient mice. Typical series of 3D stereoscopic EPR images of (a and b, green color) wild-type mice and (c and d, pink color) Nrf2-deficient mice are shown at (a and c) 5 min and (b and d) 10 min after the Carbamoyl-PROXYL injection. Nrf2-deficient mice show clearer and larger images in their hepatic and renal areas. In wild-type mice, images of the kidneys disappeared at 10 min after the Carbamoyl-PROXYL injection and the liver image was diminished. The liver and the kidneys of Nrf2-deficient mice were clearly imaged even at this time. The experimental procedures are described in Fig. 1 and in Materials and Methods.

radicals are considered to react with hydroxyl radicals or other ROS and lose their paramagnetic properties, which leads to accelerated EPR signal disappearance [13,16]. Therefore, the balance between the reducing activity of tissue and local free radical reaction determines the signal decay rate of Carbamoyl-PROXYL.

The EPR imaging analysis that we employed here demonstrated significant delay in the EPR signal decay of Carbamoyl-PROXYL in the abdominal organs of Nrf2-deficient elderly mice. The kinetic analysis of in vivo EPR showed a prolonged half-life of the probe both in Nrf2-deficient mice and aged wild-type mice. Ex vivo analysis showed decreased reducing activity of the Nrf2 liver in agreement with the in vivo study. These results demonstrate that both Nrf2 deficiency and aging synergistically induce attenuation of the renal and hepatic reducing activity. Though there remains a possibility that elder Nrf2-deficient mice show some free radical production in these organs, which accelerates the EPR signal decay, this phenomenon is considerably less prominent. On the other hand, Rem/ReOx of the kidney from the Nrf2-deficient mice showed a tendency to be higher than that of wild mice, but was not significant; and, ReOx value of Nrf2 kidney was lower than that of wild-type mice. Carbamoyl-PROXYL is water soluble and excreted to urine so that changes of renal plasma flow or glomerular filtration rate may alter its signal decay. To exclude this effect, we confirmed organ-reducing activity by ex vivo experiments. In addition to these ex vivo results, our former studies showed that (i) Nrf2-deficient female mice showed decreased creatinine clearance after 60 weeks in age, which is still older than our "elderly" mice [7]; and, (ii) kidneys have the largest reducing activity among the abdominal organs [17]. Altogether, we suggest that our results of in vivo experiments indicate decreased antioxidant activity in the kidneys.

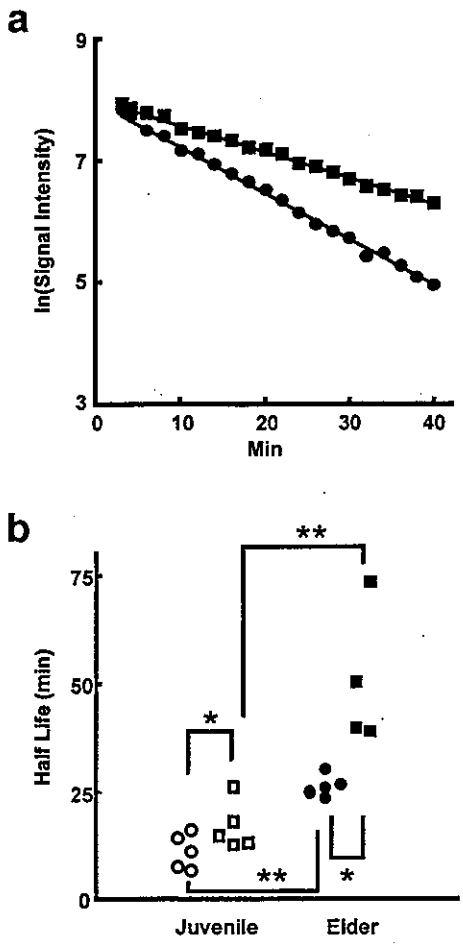

Fig. 3. Prolonged half-life of Carbamoyl-PROXYL in aged Nrf2-deficient mice. (a) Typical representative signal decay curves of Carbamoyl-PROXYL from wild-type (○) and Nrf2-deficient (□) mouse; (b) half-life of Carbamoyl-PROXYL in the upper abdominal area. Circles indicate wild-type mice and squares indicate Nrf2-deficient mice at juvenile (open) and elder (solid) stages. Signal intensities were measured every 60 s from 4 to 40 min after the Carbamoyl-PROXYL injection; (a) values are indicated at every 120 s. Note that the half-life of Carbamoyl-PROXYL decay is prolonged by Nrf2 deficiency in both juvenile and elder mice. Aging also extended the half-life of Carbamoyl-PROXYL both in the wild-type and Nrf2-deficient mice; $*p < .05$; $**p < .01$. EPR conditions were as follows: magnetic field, 37.0 ± 5.0 mT; modulation width, 0.69 mT; time constant, 0.03 s; microwave power, 0.25 mW; and scanning time, 30 s.

Table 1. Ex vivo Analysis of Organ Reduction Activity for Carbamoyl-PROXYL

	Wild-type mice	Nrf2-deficient mice
Liver		
Rem	27.9 ± 5.6	51.4 ± 31.3
ReOx	360 ± 90	310 ± 70
Rem/ReOx ($\times 10^{-2}$)	6.70 ± 0.3	11.1 ± 1.3*
Kidney		
Rem	140 ± 30	100 ± 11
ReOx	770 ± 70	440 ± 100*
Rem/ReOx ($\times 10^{-2}$)	20.7 ± 1.6	23.4 ± 5.5

Rem = the signal intensity remaining Carbamoyl-PROXYL amounts in the homogenates from the organs; ReOx = the signal intensity after the addition of potassium ferricyanide (total tissue hydroxylamine).

* Statistically significant, $p < .05$.

In the progression of lupus nephritis, ROS are considered to be important players in both direct cell injury and the pathway signaling organ damage leading to end stage renal failure [18]. Additionally, improvement of antioxidant activity by dietary supplementation with ω-3 fatty acid ameliorates the nephritis in the NZB/W model [19]. The glomerulonephritis in Nrf2-deficient mice occurs much later than in the other lupus murine models (e.g., MRL/*lpr* or NZB/W), and at the onset of this glomerulonephritis, Nrf2-deficient female mice are exposed to high oxidative stress [7]. These facts lead to a hypothesis that not only the primary damage of inflammation but also reduced antioxidant activity, caused by Nrf2 deficiency during aging, participate in the onset of the glomerulonephritis and other pathophysiological conditions such as induction of anti-DNA antibodies.

Our data show that the half-life of Carbamoyl-PROXYL of juvenile Nrf2-deficient mice was already longer than that of wild-type mice. This decreased Carbamoyl-PROXYL-reducing activity becomes remarkable in elder mice, and the Carbamoyl-PROXYL half-life in juvenile Nrf2-deficient mice is similar to that of elder wild-type mice. These results suggest a primary decrease of tissue-reducing activity in the juvenile stage and its expansion during the aging process. This deterioration of reducing activity was observed both in organs and over the total upper abdominal area, and, thus, can affect the onset of nonrenal features of lupus. Taken together with the fact that the lupus-like changes in the Nrf2-deficient mice were only observed in the elder animals, these data indicate that disturbances in tissue-repairing mechanisms due to attenuated antioxidant activity, following the initial inflammatory damage, may play a key role in the onset of lupus. Evaluation of reducing activity in combination with EPR imaging and half-life or rate constant analysis by in vivo EPR allows us in vivo, real-time, and low-invasive redox analysis, which is the most exceptional feature of EPR.

Acknowledgements — We thank Drs. H. Yokoyama, K. Oikawa, H. Ohya, and H. Kamada, Institute for Life Support Technology, Yamagata Public Corporation for the Development of Industry, for their support in EPR measurement. We also thank Prof. Guy H. Neild of University College London, Dr. Albena Dinkova-Kostova of Johns Hopkins University, and Dr. Burton D. Cohen for their help. This study was supported by the Grant-in-Aid for Scientific Research and Grant-in-Aid for Encouragement of Young Scientists from the Japan Society for the Promotion of Science and the Ministry of Education, Culture, Sports, Science, and Technology. S. T. was supported by PROBRAIN and M. Y. was supported by JSPS-RETF. A part of this work was presented at the 2002 SFRR International Meeting in Paris, and the abstract appeared in *Free Radical Biology & Medicine* previously.

REFERENCES

[1] Yoshimura, T.; Yokoyama, H.; Fujii, S.; Takayama, F.; Oikawa, K.; Kamada, H. In vivo EPR detection and imaging of endogenous nitric oxide in lipopolysaccharide-treated mice. *Nat. Biotechnol.* **14**:992–994; 1996.

[2] Itoh, K.; Chiba, T.; Takahashi, S.; Ishii, T.; Igarashi, K.; Katoh, Y.; Oyake, T.; Hayashi, N.; Satoh, K.; Hatayama, I.; Yamamoto, M.; Nabeshima, Y. An Nrf2/small Maf heterodimer mediates the induction of phase 2 detoxifying enzyme genes through antioxidant response elements. *Biochem. Biophys. Res. Commun.* **236**: 313–322; 1997.

[3] Prestera, T.; Talalay, P.; Alam, J.; Ahn, Y. I.; Lee, P. J.; Choi, A. M. Parallel induction of heme oxygenase-1 and chemoprotective phase 2 enzymes by electrophiles and antioxidants: regulation by upstream antioxidant-responsive elements (ARE). *Mol. Med.* **1**:827–837; 1995.

[4] Mulcahy, R. T.; Wartman, M. A.; Bailey, H. H.; Gipp, J. J. Constitutive and β-naphthoflavone-induced expression of the human γ-glutamylcysteine synthetase heavy subunit gene is regulated by a distal antioxidant response element/TRE sequence. *J. Biol. Chem.* **272**:7445–7454; 1997.

[5] Itoh, K.; Ishii, T.; Wakabayashi, N.; Yamamoto, M. Regulatory mechanisms of cellular response to oxidative stress. *Free Radic. Res.* **31**:319–324; 1999.

[6] Ishii, T.; Itoh, K.; Takahashi, S.; Sato, H.; Yanagawa, T.; Katoh, Y.; Bannai, S.; Yamamoto, M. Transcription factor Nrf2 coordinately regulates a group of oxidative stress-inducible genes in macrophages. *J. Biol. Chem.* **275**:16023–16029; 2000.

[7] Yoh, K.; Itoh, K.; Enomoto, A.; Hirayama, A.; Yamaguchi, N.; Kobayashi, M.; Morito, N.; Koyama, A.; Yamamoto, M.; Takahashi, S. Nrf2-deficient female mice develop lupus-like autoimmune nephritis. *Kidney Int.* **60**:1343–1353; 2001.

[8] Murphy, E. D.; Roth, J. B. Autoimmunity and lymphoproliferation: induction by mutant gene *lpr* and acceleration by a male-associated factor in strain BXSB mice. In: Rose, N. R.; Bigazzi, P. E.; Warner, N. L., eds. *Genetic control of autoimmune disease.* New York: Elsevier North Holland; 1978:207–221.

[9] Howie, J. B.; Helyer, B. J. The immunology and pathology of NZB mice. *Adv. Immunol.* **9**:215–266; 1968.

[10] Togashi, H.; Matsuo, T.; Shinzawa, H.; Takeda, Y.; Shao, L.; Oikawa, K.; Kamada, H.; Takahashi, T. Ex vivo measurement of tissue distribution of a nitroxide radical after intravenous injection and its in vivo imaging using a rapid scan ESR-CT system. *Magn. Reson. Imaging* **18**:151–156; 2000.

[11] Nishino, N.; Yasui, H.; Sakurai, H. In vivo L-band ESR and quantitative pharmacokinetic analysis of stable spin probes in rats and mice. *Free Radic. Res.* **31**:35–51; 1999.

[12] Utsumi, H.; Ichikawa, K.; Takeshita, K. In vivo ESR measurements of free radical reactions in living mice. *Toxicol. Lett.* **82–83**:561–565; 1995.

[13] Miura, Y.; Ozawa, T. Noninvasive study of radiation-induced oxidative damage using in vivo electron spin resonance. *Free Radic. Biol. Med.* **28**:854–859; 2000.

[14] Takeshita, K.; Utsumi, H.; Hamada, A. ESR measurement of radical clearance in lung of whole mouse. *Biochem. Biophys. Res. Commun.* **177**:874–880; 1991.

[15] Kuppusamy, P.; Li, H.; Ilangovan, G.; Cardounel, A. J.; Zweier, J. L.; Yamada, K.; Krishna, M. C.; Mitchell, J. B. Noninvasive imaging of tumor redox status and its modification by tissue glutathione levels. *Cancer Res.* **62**:307–312; 2002.

[16] Han, J. Y.; Takeshita, K.; Utsumi, H. Noninvasive detection of hydroxyl radical generation in lung by diesel exhaust particles. *Free Radic. Biol. Med.* **30**:516–525; 2001.

[17] Ueda, A.; Yokoyama, H.; Nagase, S.; Hirayama, A.; Koyama, A.; Ohya, H.; Kamada, H. In vivo temporal EPR imaging for estimating the kinetics of a nitroxide radical in the renal parenchyma and pelvis in rats. *Magn. Reson. Imaging* **20**:77–82; 2002.

[18] Grande, J. P. Mechanisms of progression of renal damage in lupus nephritis: pathogenesis of renal scarring. *Lupus* **7**:604–610; 1998.

[19] Chandrasekar, B.; Fernandes, G. Decreased proinflammatory cytokines and increased antioxidant enzyme gene expression by ω-3 lipids in murine lupus nephritis. *Biochem. Biophys. Res. Commun.* **200**:893–898; 1994.

ABBREVIATIONS

ARE/EpRE—antioxidant-responsive element/electrophile-responsive element

Carbamoyl-PROXYL—3-carbamoyl-2,2,5,5-tetramethylpyrrolidine-1-oxyl

EPR—electron paramagnetic resonance

HO-1—heme oxygenase-1

Nrf2—NF-E2-related factor 2

Rem—remaining Carbamoyl-PROXYL (see Materials and Methods)

ReOx—total tissue hydroxylamine (see Materials and Methods)

ROS—reactive oxygen species

Available online at www.sciencedirect.com
SCIENCE DIRECT®
Biochemical and Biophysical Research Communications 303 (2003) 105–111
BBRC
www.elsevier.com/locate/ybbrc

Gene expression of detoxifying enzymes in AhR and Nrf2 compound null mutant mouse☆

Shuhei Noda,[a,1] Nobuhiko Harada,[a,1] Azumi Hida,[a] Yoshiaki Fujii-Kuriyama,[a] Hozumi Motohashi,[a,*] and Masayuki Yamamoto[a,b]

[a] *Center for Tsukuba Advanced Research Alliance, University of Tsukuba, 1-1-1 Tennoudai, Tsukuba 305-8577, Japan*
[b] *ERATO Environmental Response Project, Japan Science and Technology Corporation, 1-1-1 Tennoudai, Tsukuba 305-8577, Japan*

Received 10 February 2003

Abstract

The arylhydrocarbon receptor (AhR) regulates the expression of cytochrome P450 (CYP)-1 gene family members which catalyze xenobiotic Phase I metabolism, while Nrf2 exerts the concerted regulation of Phase II enzyme genes. We generated AhR and Nrf2 compound null mutant mice to examine the integrated function of AhR- and Nrf2-regulated enzymes in detoxification. Furthermore, we used this mouse model, by administering three different classes of chemical inducers, to examine how xenobiotic metabolism may be influenced in the absence of signals transduced by AhR or Nrf2. The compound mutant mice responded only weakly to AhR ligand or Phase II inducer, while they displayed a clear response to phenobarbital, an inducer of the CYP2B family through another, unrelated transcription factor. Here, we report an initial characterization of the AhR-Nrf2 double mutant mice, which may serve as a simplified bioassay system to evaluate xenobiotic toxicity and metabolic biotransformation of various drugs and environmental chemicals.

Keywords: Xenobiotics; Phase I enzymes; Phase II enzymes; Gene knockout mouse; 3-Methylchoranthrene; Butylated hydroxyanisole; Phenobarbital

The detoxification of foreign substances, although complex, can be considered to comprise two sequential reaction processes; namely, Phase I and Phase II. In Phase I reactions, foreign chemicals are mainly oxidized by cytochrome P450 (CYP) enzymes to become polarized metabolites. Subsequently, Phase II metabolism, catalyzed by enzymes such as glutathione *S*-transferase (GST) and NAD(P)H:quinone oxidoreductase (NQO1), converts the reactive Phase I products to more hydrophilic substances [1].

Four members of the *CYP* gene family, i.e., *CYP1–CYP4*, encode liver-expressed enzymes responsible for metabolizing xenobiotics and endogenous lipophilic substrates. The transcription of many members of the CYP1–CYP4 family can be activated by foreign chemicals through one of the four receptor-dependent mechanisms. The aryl hydrocarbon receptor (AhR) is a basic region-helix-loop-helix (bHLH)-PAS transcription factor that regulates the *CYP1* family genes. When bound by polycyclic aromatic hydrocarbons (PAHs), such as dioxins and 3-methylchoranthrene (3-MC), AhR translocates from the cytoplasm to the nucleus, heterodimerizes with AhR nuclear translocator (ARNT), and activates transcription through the xenobiotic-responsive element (XRE) [2]. The requirement for the AhR in the inducible expression of *CYP1* family genes by PAH was demonstrated in AhR-null mutant mice, which were generated independently by three different laboratories [3–5].

☆ *Abbreviations:* CYP, cytochrome P450; 3-MC, 3-methylchoranthrene; BHA, butylated hydroxyanisole; *t*-BHQ, *tert*-butylhydroquinone; PB, phenobarbital; AhR, aryl hydrocarbon receptor; ARNT, AhR nuclear translocator; Nrf2, nuclear factor-erythroid 2 p45-related factor 2; CAR, constitutive androstane receptor; XRE, xenobiotic-responsive element; ARE, antioxidant-responsive element; GST-P, glutathione *S*-transferase class Pi; NQO1, NAD(P)H:quinone oxidoreductase 1; D-KO, double knockout mouse of AhR and Nrf2; N-KO, Nrf2 knockout mouse; A-KO, AhR knockout mice; WT, wild type.

* Corresponding author. Fax: +81-29-853-7318.
E-mail address: hozumim@tara.tsukuba.ac.jp (H. Motohashi).

[1] These authors equally contributed to this work.

0006-291X/03/$ - see front matter © 2003 Elsevier Science (USA). All rights reserved.
doi:10.1016/S0006-291X(03)00306-1

The xenobiotic induction mechanism of CYP2, 3, and 4 involves three distinct orphan nuclear receptors. CYP2B induction by phenobarbital (PB) and other PB-like lipophilic chemicals is mediated by the constitutive androstane receptor (CAR) through its interaction with the PB-responsive enhancer module (PBREM) [6]. Germ line mutation of the murine *CAR* gene revealed that it is essential for the PB-induction of the *CYP2B* family of genes [7]. PXR activates the *CYP3A* family genes in response to diverse chemicals including natural and synthetic steroids [8], whereas PPAR mediates the induction of the *CYP4A* family genes by many acidic chemicals classified as non-genotoxic carcinogens and peroxisome proliferators [9].

The genes of Phase II metabolism are also regulated in a concerted manner at the transcriptional level through the antioxidant-responsive element (ARE) or electrophile-responsive element (EpRE) [10,11]. Our previous analysis of nrf2-null mutant mice revealed that Nrf2 is central to ARE-mediated gene expression [12]. Nrf2 belongs to a family of transcription factors containing a basic region-leucine zipper (bZip) motif. The products of Phase I metabolism, as well as Phase II inducers, such as butylated hydroxyanisole (BHA) and Oltipraz, cause Nrf2 to dissociate from a cytoplasmic inhibitor molecule called Keap1, thereby permitting Nrf2 to translocate into the nucleus [13]. Nrf2 activates transcription of Phase II genes through the ARE/EpRE. In the absence of Nrf2, Phase II inducers were ineffective [14], and consequently, the reactive Phase I metabolites are not conjugated for excretion but form electrophiles that may attack intracellular macromolecules including DNA and protein [15,16].

To establish a model mouse system for assessing the integrated function of the AhR battery and Nrf2 battery in detoxification and to understand the contribution of AhR and Nrf2 to xenobiotic metabolism, we generated AhR–Nrf2 compound null mutant mice. Initial characterization of the double mutant mice focused on their responsiveness to three chemicals of different categories, 3-MC as a model AhR ligand, BHA as an activator of Nrf2, and PB as a regulator of the *CYP2B* family genes. Genes for CYP1A1, CYP1A2, NQO1, GST-P, and CYP2B10 were selected for analysis. The AhR–Nrf2 compound null mutant mice respond to neither the AhR ligand nor the Phase II inducer, while they displayed a clear response to PB. Thus, the AhR–Nrf2 double mutant mice serve as a simplified bioassay system for PB and related chemicals under conditions free of AhR and Nrf2 interference.

Materials and methods

Generation of $AhR^{-/-}$::$Nrf2^{-/-}$ mice. AhR- and Nrf2-null mutant mice were previously generated [5,12]. After the crossing of $AhR^{-/-}$ male mouse in 129svJ-C57BL/6 mixed background and a $Nrf2^{-/-}$ female mouse in 129svJ-ICR mixed background, the mice heterozygous for both genes ($AhR^{-/+}$::$Nrf2^{-/+}$) were obtained. One male and two females from the same litter were further intercrossed to produce progeny null for both AhR and Nrf2 genes. Double heterozygous ($AhR^{-/+}$::$Nrf2^{-/+}$) and double homozygous ($AhR^{-/-}$::$Nrf2^{-/-}$) mutant mice obtained from the offspring were bred for 400 days to examine their survival. The double homozygous female animals (D-KO) were exploited for enzyme-induction experiments with chemical inducers at 3–6 months after birth together with the control wild-type (WT), Nrf2 single homozygous (N-KO), and AhR single homozygous (A-KO) females at the same age.

Animals were housed under controlled temperature (23 °C), humidity (40–60%), and lighting (14/10 h light/dark cycle) and provided food (Oriental Yeast, Tokyo) and water ad libitum. AhR genotype was determined by PCR with three primers (5′-CGCGGGCACCATGAGCAG-3′, 5′-TTGAGACTCAGCTCCTGGATGG-3′, 5′-GCGGATTGACCGTAATGGGATAGG-3′) under the condition of 96 °C for 20 s, 62 °C for 30 s, and 72 °C for 45 s. For PCR of Nrf2 genotyping, three primers (5′-TGGACGGGACTATTGAAGGCTG-3′, 5′-GCCGCCTTTTCAGTAGATGGAGG-3′, 5′-GCGGATTGACCGTAATGGGATAGG-3′) were used at 96 °C for 20 s, 59 °C for 30 s, and 72 °C for 45 s.

Survival curve. Cohorts of 32 $AhR^{-/+}$::$Nrf2^{-/+}$ mice and of 65 D-KO mice were followed for 400 days to see their survival. Data were plotted into Kaplan–Meier survival curves.

Treatment with chemical inducers. 3-MC (WAKO Pure Chemical, Tokyo) was administered intraperitoneally at a dose of 80 mg/kg dissolved in corn oil as vehicle. Oral gavage treatment was employed to administer BHA (Sigma, Darmstadt) at a dose of 400 mg/kg dissolved in corn oil as vehicle. PB (Tokyo Kasei Kougyo, Tokyo) was injected intraperitoneally at a dose of 80 mg/kg in saline once a day for three consecutive days. The animals were sacrificed 24 h after the last treatment and the liver was processed for RNA purification.

RNA blot analysis. Total RNA was isolated from the liver with Isogen (Nippon Gene, Toyama) according to the manufacturer's instruction. Fifteen micrograms of purified total RNA was denatured and separated on 1% agarose gel containing formaldehyde, followed by capillary transfer to a nylon membrane (Zeta Probe Blotting Membrane; Bio-Rad Laboratories, CA). cDNA fragments of CYP1A1, CYP1A2, NQO1, GST-P, CYP2B10, and G3PDH were labeled and used as probes. Hybridization and washing were performed under the instruction manual of Zeta Probe Blotting Membrane.

Results and discussion

Generation of $AhR^{-/-}$::$Nrf2^{-/-}$ compound mutant mice

$AhR^{-/-}$ male mice and $Nrf2^{-/-}$ female mice were mated to obtain $AhR^{+/-}$::$Nrf2^{+/-}$ double heterozygous mice. $AhR^{-/-}$::$Nrf2^{-/-}$ compound mutant mice were generated from the mating of double heterozygous animals. Approximately half of the double homozygous mutant (D-KO) mice died within one week after birth for unknown reason(s), but the mice that survived this critical period became stable (below). The survival rate was 40% after 400 days (Fig. 1). When pups were examined one week after birth, no significant changes were observed except for the liver, where steatosis developed as previously reported in the analysis of AhR-null mutant mice [4].

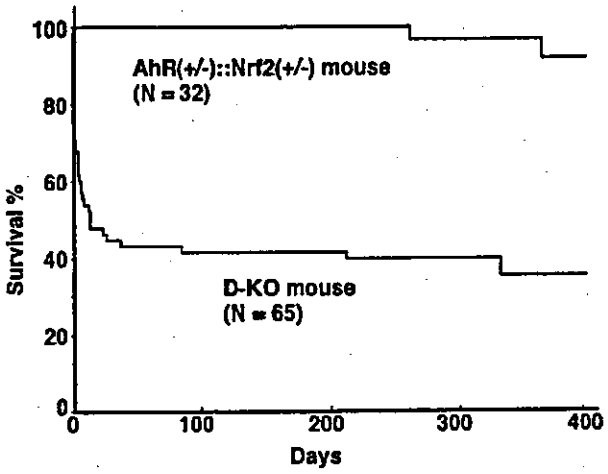

Fig. 1. Long-term survival of the D-KO mice. Sixty-five D-KO (double homozygous) mice and 32 control double heterozygous mice were bred up to 400 days. Survival ratios of each genetic group were plotted into Kaplan–Meier curves.

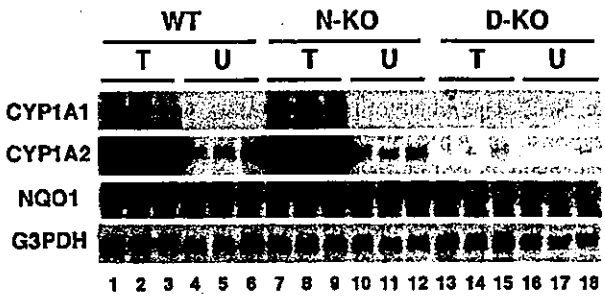

Fig. 2. Expression profiles of detoxifying enzyme genes in WT, N-KO, and D-KO mice induced by 3-MC. WT, N-KO, and D-KO were treated with 3-MC or vehicle as described in Materials and methods. Total RNAs (15 μg) extracted from the liver were subjected to RNA blot analysis. The expression levels of CYP1A1, CYP1A2, and NQO1 mRNAs were examined together with G3PDH mRNA as a loading control. WT mice treated with 3-MC (lanes 1–3) or vehicle (lanes 4–6), N-KO mice treated with 3-MC (lanes 7–9) or vehicle (lanes 10–12), and D-KO mice treated with 3-MC (lanes 13–15) or vehicle (lanes 16–18) were examined. T, treated; U, untreated.

The D-KO survivors, both males and females, were viable and fertile and displayed no apparent phenotypic change. We therefore examined carefully their major organs, including brain, heart, lung, thymus, stomach, intestine, spleen, liver, kidney, bladder, and reproductive organs, both macroscopically and microscopically, but again we could find no apparent abnormalities (data not shown). We envisage that heterogeneity in the genetic background might affect the neonatal viability of each D-KO mouse. However, most importantly for this study, obtaining viable D-KO mice enabled us to analyze the xenobiotic response in a situation where the *AhR* and *Nrf2* genes are simultaneously ablated.

Response to 3-methylchoranthrene

We first treated the D-KO mice with 3-MC, which induces Phase I gene expression through the XRE. Since AhR-null mutant (A-KO) animals have already been reported to be unresponsive to 3-MC treatment [17], we compared the 3-MC response in D-KO animals to those of Nrf2-null mutant (N-KO) and wild type (WT) mice. The expression levels of *CYP1A1*, *CYP1A2*, and *NQO1* genes were examined, which are categorized as the "AhR battery" [18]. The inducible expression of the *CYP1A1* and *CYP1A2* genes was completely abolished in the D-KO mice (Fig. 2, lanes 13–18), while the N-KO mice (Fig. 2, lanes 7–12) displayed a normal response comparable to those of WT mice (Fig. 2, lanes 1–6). This result is consistent with previous reports showing that *CYP1A1* and *CYP1A2* are typical AhR target genes [19,20], and demonstrates that the induction of CYP1A family genes by 3-MC is independent of Nrf2.

In contrast, the gene induction of *NQO1* was abolished both in the N-KO mice and D-KO mice (Fig. 2). This results shows that Nrf2 is indispensable for the induction of *NQO1* gene by 3-MC. Although the *NQO1* gene has been included in the "AhR battery," some controversy remains regarding its regulatory mechanism [21]. It has been shown that *NQO1* gene expression is strongly induced in C57BL/6 mice possessing high affinity AhR, but not in DBA/2 mice possessing low affinity AhR [22], suggesting that the induction of NQO1 by 3-MC correlates with AhR activity. The existence of an XRE motif in the upstream regulatory region of the *NQO1* gene supports the conclusion of this observation [21]. However, the true significance of the XRE motif for the gene expression has not yet been established. Importantly, the regulatory region of the *NQO1* gene also contains an ARE, and one report showed that the ARE, not the XRE, is critical for NQO1 induction by TCDD (2,3,7,8-tetrachlorodibenzo-*p*-dioxin), a model AhR ligand [23].

A plausible mechanism whereby AhR ligands induce expression of the *NQO1* gene may involve an increase in oxidative stress capable of promoting Nrf2 activation, which in turn could increase the expression of the *NQO1* gene. Consistent with this view, the *GST-P* gene, a recognized ARE-dependent gene, shows a similar pattern of gene induction by 3-MC (data not shown). An alternative possibility is that the AhR activates *NQO1* gene transcription synergistically with Nrf2, although no report has shown that Nrf2 activity depends on the availability of the AhR in the neighboring XRE.

Response to BHA

BHA is a mono-functional inducer of detoxifying enzymes, capable of inducing Phase II enzymes but not Phase I enzymes. This ability of BHA to induce Phase II gene expression may result from its oxidative

metabolism to several active polar species including *t*-BHQ (*tert*-butylhydroquinone) as it has been reported to occur in the presence of microsomes [24]. To confirm the Nrf2-dependency of BHA action, we examined the response of AhR–Nrf2 double mutant mice to BHA treatment in comparison to those of WT, N-KO, and A-KO animals. WT and N-KO mice were obtained as littermates of D-KO mice from the double heterozygous mating, whereas A-KO mice were prepared independently from different parents due to breeding problems in the original mating.

NQO1 and *GST-P* were chosen as typical genes activated by BHA administration. In accordance with our expectation, the expression level of *NQO1* mRNA was clearly increased in the livers of WT and A-KO mice by 5.5- and 3.0-fold, respectively (Fig. 3, lanes 19–30), but induction was abolished in the N-KO and D-KO mouse livers (Fig. 3, lanes 1–18). *GST-P* mRNA was strongly induced 14- and 4.6-fold in WT and A-KO mice (Fig. 3, lanes 19–30), but weakly induced 1.6- and 2.0-fold in N-KO and D-KO mice, respectively (Fig. 3, lanes 1–18). These results confirm the fact that Nrf2 makes a major contribution to the inducible expression of *NQO1* and *GST-P* genes. It is interesting that in the A-KO mice

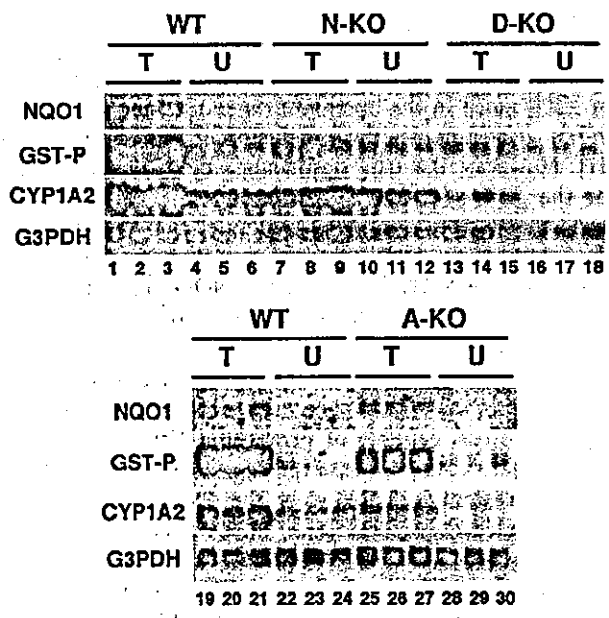

Fig. 3. Expression profiles of detoxifying enzyme genes induced in WT, N-KO, D-KO, and A-KO mice by BHA. WT, N-KO, D-KO, and A-KO mice were treated with BHA or vehicle. Total RNAs (15 μg) extracted from the liver were subjected to RNA blot analysis. The expression levels of NQO1, GST-P, and CYP1A2 mRNAs were examined together with G3PDH mRNA as a loading control. WT mice treated with BHA (lanes 1–3, 19–21) or vehicle (lanes 4–6, 22–24), N-KO mice treated with BHA (lanes 7–9) or vehicle (lanes 10–12), D-KO mice treated with BHA (lanes 13–15) or vehicle (lanes 16–18), and A-KO mice treated with BHA (lanes 25–27) or vehicle (lanes 28–30) were examined. T, treated; U, untreated.

there was a 45% (from 5.5- to 3.0-fold) decrease in *NQO1* induction and 67% (from 14- to 4.6-fold) decrease in *GST-P* induction. This may reflect an inability of the A-KO mice to metabolize BHA to active metabolites, such as *t*-BHQ, and suggests that, in vivo, AhR-dependent *CYP* genes make an active contribution to the metabolism of BHA. It further suggests that *GST-P* induction is partially mediated by mechanisms independent of both AhR and Nrf2.

CYP1A2 is a known Phase I enzyme but was induced by BHA treatment in all the mice examined (Fig. 3). The relative induced expression levels of *CYP1A2* gene are 1.0, 0.73, 0.17, and 0.29 in WT, N-KO, D-KO, and A-KO mice, respectively (Fig. 3, lanes 1–3, 7–9, 13–15, 19–21, and 25–27). They are the highest in WT, intermediate in N-KO and in A-KO, and the lowest in D-KO. This result suggests that both Nrf2 and AhR are necessary for the higher levels of the induced expression of the *CYP1A2* gene. The relative basal expression levels are 1.0, 1.0, 0.1, and 0.3 in WT, N-KO, D-KO, and A-KO mice, respectively (Fig. 3, lanes 4–6, 10–12, 16–18, 22–24, and 28–30). They are high in WT and N-KO, and low in D-KO and A-KO. This result indicates that the AhR is critical for maintaining the basal expression levels of the *CYP1A2* gene.

When the *CYP1A2* locus in the mouse genomic database was examined, several AREs and XREs were found in the sequence surrounding the *CYP1A2* gene (data not shown). Although none of the AREs have been experimentally tested, we surmise that some of the AREs in this locus might be responsible for the gene activation by BHA. On the contrary, XREs within this locus were well examined and characterized. Since several XREs are present in the mouse *CYP1A2* locus and the corresponding human locus [25], the AhR may, through the XREs, direct basal levels of expression of the *CYP1A2* gene in addition to its induction. However, from an analysis of the human *CYP1A2* gene in a transient overexpression assay, no apparent XRE was found within the regions important for basal constitutive transcription [26], whereas functional XREs were identified in the upstream regions required for the response to 3-MC [20]. Assuming that the regulatory mechanisms are conserved between human and mouse, the contribution made by the AhR to the constitutive expression of the*CYP1A2* gene might be indirect.

Response to PB

PB activates transcription of the *CYP2B* family of genes. This induction has been shown to be under the regulation of CAR transcription factor and PBREM sequence [6]. In this study, we examined how the lack of both AhR and Nrf2 affects the PB-mediated induction of CYP2B10. We found that *CYP2B10* gene expression was induced in the liver of mice of all genotypes tested

(Fig. 4). However, the relative induced expression levels are 1.0, 0.6, 4.1, and 2.9 in WT, N-KO, D-KO, and A-KO, respectively (Fig. 4, lanes 1–3, 7–9, 13–15, 19–21, and 25–27). The magnitude of induction is far greater in A-KO and D-KO than in WT and N-KO mice, indicating that the *AhR* gene disruption leads to the super-induction of *CYP2B10* gene expression. This result indicates that AhR directly or indirectly represses the PB-mediated induction of *CYP2B10* gene.

One possible explanation is an indirect effect of AhR disruption. PB metabolism may be retarded in the absence of AhR, resulting in the higher effective PB concentration in A-KO and D-KO livers. Supporting this contention, an elongated sedative effect of PB was observed in D-KO and A-KO animals (data not shown).

Alternative explanation would be a rather direct repressive effect of AhR on *CYP2B10* gene transcription. It is intriguing to note two recent reports related to the regulation of *CYP2B* family genes, in which transcriptional coactivator SRC-1 was reported to enhance the AhR transcriptional activity [27] and also to potentiate the CAR activity for the transcription of the rat *CYP2B1* gene [28]. The AhR potentiation appears to be the consequence of direct interaction of SRC-1 and AhR [27] or SRC-1 and ARNT [29], while the CAR potentiation requires flanking regions of PBREM core sequence as well as the core sequence itself, suggesting the requirement of additional factor(s) for the enhancement of CAR activity by SRC-1 coactivator [28]. These studies thus imply that AhR and CAR share or compete for the common coactivator SRC-1, which may explain the super-induction of the *CYP2B10* gene expression by PB in the absence of AhR.

We found that the *CYP1A2* gene was also induced by PB in all the mice examined 1.8-, 2.6-, 5.5-, and 4.4-fold in WT, N-KO, D-KO, and A-KO, respectively (Fig. 4). This result indicates that both AhR and Nrf2 are dispensable for the inducible expression of the *CYP1A2* gene by PB. The higher fold induction in the absence of AhR (D-KO and A-KO) is attributed to the lower basal expression levels (discussed above). Recent report showed that the *CYP1A2* induction by PB is abolished in the CAR-null mutant mice [30]. Since the mechanism of PB-mediated induction of *CYP1A2* gene has not been elucidated yet, we examined the mouse *CYP1A2* gene locus in the database for PBREM. We found one PBREM consensus sequence at 2.6-kbp upstream of the transcription initiation site and are planning to test the significance of this element for the PB-mediated induction of the *CYP1A2* gene. The *CYP1A2* induction is suggested to be one cause for the increased acetaminophen toxicity by pretreatment with PB [30].

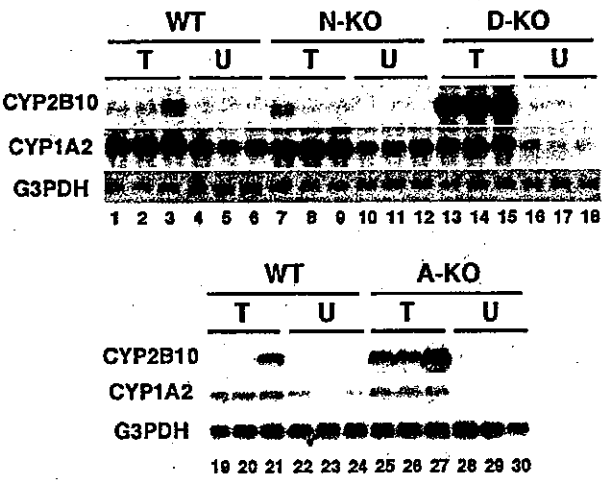

Fig. 4. Expression profiles of detoxifying enzyme genes induced in WT, N-KO, D-KO, and A-KO mice by PB. WT, N-KO, D-KO, and A-KO mice were treated with PB or vehicle. Total RNAs (15 μg) extracted from the liver were subjected to RNA blot analysis. The expression levels of CYP2B10 and CYP1A2 mRNAs were examined together with G3PDH mRNA. WT mice treated with PB (lanes 1–3, 19–21) or vehicle (lanes 4–6, 22–24), N-KO mice treated with PB (lanes 7–9) or vehicle (lanes 10–12), D-KO mice treated with PB (lanes 13–15) or vehicle (lanes 16–18), and A-KO mice treated with PB (lanes 25–27) or vehicle (lanes 28–30) were examined. T, treated; U, untreated.

Prospective uses of AhR$^{-/-}$::Nrf2$^{-/-}$ compound mutant mice

As a mouse model, the AhR–Nrf2 D-KO mouse line could find applications in numerous fields including pharmacology and environmental and agricultural toxicology. In this study, we established an AhR–Nrf2 D-KO mouse line and confirmed that these mice lack the ability to respond to both 3-MC and BHA, a typical AhR ligand and a Phase II inducer, respectively (Fig. 5). It is conceivable that the D-KO mice are virtually devoid of the major PAH-metabolizing pathway. As our aim

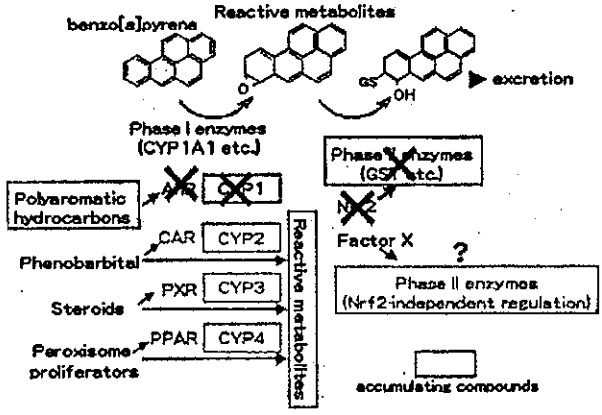

Fig. 5. Schematic illustration of the metabolic and detoxifying pathways remaining in D-KO mice. AhR- or Nrf2-dependent response is abolished and the disrupted pathways are colored in blue. The remaining pathways independent of AhR and Nrf2 function are colored in red. Compounds accumulating in D-KO mice are surrounded by green squares.

was to exploit the D-KO mice in toxicological and pharmacological studies, we wish to propose here some possible applications for the AhR–Nrf2 D-KO mutant animals (Fig. 5). Using this mouse model it would be possible to clarify the contribution that the AhR battery and Nrf2 battery genes make to the detoxification pathway. Further, an analysis of xenobiotic metabolism could be made in the absence of the gene inductions, normally directed by AhR and Nrf2.

An interesting aspect of the analysis of the D-KO mouse is the change in the metabolic pathway of various xenobiotic or pharmaceutical compounds. We are curious about the qualitative and quantitative alteration of metabolites in each organ. Observed changes in the metabolism of xenobiotics in the D-KO mice could reveal the integrated and coordinated functions of the AhR-regulated genes and the Nrf2-regulated genes to the detoxification processes.

This mouse model could also simplify investigations into the gene-induction response of regulators other than AhR–Nrf2, unveiling novel process that may otherwise be buried under major pathways of metabolism. Another tempting experiment is to use the D-KO mice to test the effect of chronic toxicity by PAHs. The PAHs should accumulate within the body of D-KO mice over long periods of time, since in theory PAHs should only be slowly metabolized in the absence of AhR and Nrf2.

Concluding remarks

Ingestion of numerous, sometimes harmful, xenobiotics is inevitable. Even food naturally contains many compounds requiring detoxification, in addition to artificial chemicals used in the growing and processing of foodstuffs, such as remnants of agricultural pesticides. Inhalation of air pollutants from combusted fuel and the emissions from factories account for further exposure to toxic chemicals. Therefore, a growing need exits to develop a human-oriented bioassay system capable of evaluating the toxicity of xenobiotics with reasonable sensitivity and specificity. Our $AhR^{-/-}$::$Nrf2^{-/-}$ compound mutant mouse line should provide such a unique and effective assay system in toxicological evaluations.

Acknowledgments

We are grateful to Drs. Vincent Kelley, Tomonori Hosoya, Jun-sei Mimura, and Satoru Takahashi for discussion, and Masahiko Negishi for CYP2B10 cDNA. We thank Ms. Naomi Kaneko for histological analysis and Reiko Kawai for mouse breeding. This work was supported by grants from ERATO (M.Y.), the Ministry of Education, Science, Sports and Culture (H.M. and M.Y.), JSPS-RFTF (M.Y.), CREST (M.Y. and Y.F.-K.), PROBRAIN (H.M.), and Special Coordination Fund for Promoting Science and Technology (H.M.).

References

[1] P. Talalay, Mechanisms of induction of enzymes that protect against chemical carcinogenesis, Adv. Enzyme Regul. 28 (1989) 237–250.
[2] K. Sogawa, Y. Fujii-Kuriyama, Ah receptor, a novel ligand-activated transcription factor, J. Biochem. (Tokyo) 122 (1997) 1075–1079.
[3] P.M. Fernandez-Salguero, T. Pineau, D.M. Hilbert, T. McPhail, S.S. Lee, S. Kimura, D.W. Nebert, S. Rudikoff, J.M. Ward, F.J. Gonzalez, Immune system impairment and hepatic fibrosis in mice lacking the dioxin-binding Ah receptor, Science 268 (1995) 722–726.
[4] J.V. Schmidt, G.H. Su, J.K. Reddy, M.C. Simon, C.A. Bradfield, Characterization of a murine Ahr null allele: involvement of the Ah receptor in hepatic growth and development, Proc. Natl. Acad. Sci. USA 93 (1996) 6731–6736.
[5] J. Mimura, K. Yamashita, K. Nakamura, M. Morita, T.N. Takagi, K. Nakao, M. Ema, K. Sogawa, M. Yasuda, M. Katsuki, Y. Fujii-Kuriyama, Loss of teratogenic response to 2,3,7,8-tetrachlorodibenzo-*p*-dioxin (TCDD) in mice lacking the Ah (dioxin) receptor genes, Genes Cells 2 (1997) 645–654.
[6] P. Honkakoski, I. Zelko, T. Sueyoshi, M. Negishi, The nuclear orphan receptor CAR-retinoid X receptor heterodimer activates the phenobarbital-responsive enhancer module of the CYP2B gene, Mol. Cell. Biol. 18 (1998) 5652–5658.
[7] P. Wei, J. Zhang, M. Egan-Hafley, S. Liang, D.D. Moore, The nuclear receptor CAR mediates specific xenobiotic induction of drug metabolism, Nature 407 (2000) 920–923.
[8] S.A. Kliewer, J.T. Moore, L. Wade, J.L. Staudinger, M.A. Watson, S.A. Jones, D.D. McKee, B.B. Oliver, T.M. Willson, R.H. Zetterstrom, T. Perlmann, J.M. Lehmann, An orphan nuclear receptor activated by pregnanes defines a novel steroid signaling pathway, Cell 92 (1998) 73–82.
[9] A.C. Bayly, N.J. French, C. Dive, R.A. Roberts, Non-genotoxic hepatocarcinogenesis in vitro: the FaO hepatoma line responds to peroxisome proliferators and retains the ability to undergo apoptosis, J. Cell Sci. 104 (1993) 307–315.
[10] R.S. Friling, A. Bensimon, T. Tichauer, V. Danial, Xenobiotic-inducible expression of murine gluthatione *S*-transferase Ya subunit gene is controlled by as electrophile-responsive element, Proc. Natl. Acad. Sci. USA 87 (1990) 6258–6262.
[11] T.H. Rushmore, M.R. Morton, C.B. Pickett, The antioxidant responseive element. Activation by oxidative stress and identification of the DNA consensus sequence required for functional activity, J. Biol. Chem. 266 (1991) 11632–11639.
[12] K. Itoh, T. Chiba, S. Takahashi, T. Ishii, K. Igarashi, Y. Katoh, T. Oyake, N. Hayashi, K. Satoh, I. Hatayama, An Nrf2/small Maf heterodimer mediates the induction of phase II detoxifying enzyme genes through antioxidant response elements, Biochem. Biophys. Res. Commun. 236 (1997) 313–322.
[13] K. Itoh, N. Wakabayashi, Y. Katoh, T. Ishii, K. Igarashi, J.D. Engel, M. Yamamoto, Keap1 represses nuclear activation of antioxidant responsive elements by Nrf2 through binding to the amino-terminal Neh2 domain, Genes Dev. 13 (1999) 76–86.
[14] M. McMahon, K. Itoh, M. Yamamoto, S.A. Chanas, C.J. Henderson, L.I. McLellan, C.R. Wolf, C. Cavin, J.D. Hayes, The cap'n'collar basic leucine zipper transcription factor Nrf2 (NF-E2 p45-related factor 2) controls both constitutive and inducible expression of intestinal detoxification and glutathione biosynthetic enzymes, Cancer Res. 61 (2001) 3299–3307.
[15] A. Enomoto, K. Itoh, E. Nagayoshi, J. Haruta, T. O'Connor, T. Harada, M. Yamamoto, High sensitivity of Nrf2 knockout mice to acetoaminophen hepatotoxicity associated with decreased expression of ARE-regulated drug metabolizing enzymes and antioxidant genes, Toxicol. Sci. 59 (2001) 169–177.

[16] Y. Aoki, H. Sato, N. Nishimura, S. Takahashi, K. Itoh, M. Yamamoto, Accelerated DNA adduct formation in the lung of the Nrf2 knockout mouse exposed to diesel exhaust, Toxicol. Appl. Pharmacol. 173 (2001) 154–160.

[17] T. Shimada, K. Inoue, Y. Suzuki, T. Kawai, E. Azuma, T. Nakajima, M. Shindo, K. Kurose, A. Sugie, Y. Yamagishi, Y. Fujii-Kuriyama, M. Hashimoto, Arylhydrocarbon receptor-dependent induction of liver and lung cytochromes P450 1A1, 1A2, and 1B1 by polycyclic aromatic hydrocarbons and polychlorinated biphenyls in genetically engineered C57BL/6J mice, Carcinogenesis 23 (2002) 1199–1207.

[18] D.W. Nebert, A.L. Roe, M.Z. Dieter, W.A. Solis, Y. Yang, T.P. Dalton, Role of the aromatic hydrocarbon receptor and [Ah] gene battery in the oxidative stress response, cell cycle control, and apoptosis, Biochem. Pharmacol. 59 (2000) 65–85.

[19] A. Fujisawa-Sehara, M. Yamane, Y. Fujii-Kuriyama, A DNA-binding factor specific for xenobiotic responsive elements of P-450c gene exists as a cryptic form in cytoplasm: its possible translocation to nucleus, Proc. Natl. Acad. Sci. USA 85 (1988) 5859–5863.

[20] L.C. Quattrochi, T. Vu, R.H. Tukey, The human CYP1A2 gene and induction by 3-methylchoranthrene. A region of DNA that supports AH-receptor binding and promoter-specific induction, J. Biol. Chem. 269 (1994) 6949–6954.

[21] L.V. Favreau, C.B. Pickett, Transcriptional regulation of the rat NAD(P)H:quinone reductase gene. Identification of regulatory elements controlling basal level expression and inducible expression by planar aromatic compounds and phenolic antioxidants, J. Biol. Chem. 266 (1991) 4556–4561.

[22] J.A. Robertson, H.C. Chen, D.W. Nebert, NAD(P)H:menadione oxidoreductase. Novel purification of enzyme cDNA and complete amino acid sequence, and gene regulation, J. Biol. Chem. 261 (1986) 15797–15799.

[23] V. Radjendirane, A.K. Jaiswal, Antioxidant response element-mediated 2,3,7,8-tetrachlorodibenzo-*p*-dioxin (TCDD) induction of human NAD(P)H:quinone oxidoreductase 1 gene expression, Biochem. Pharmacol. 58 (1999) 1649–1655.

[24] S.W. Cummings, G.A. Ansari, F.P. Guengerich, L.S. Crouch, R.A. Prough, Metabolism of 3-*tert*-butyl-4-hydroxyanisole by microsomal fractions and isolated rat hepatocytes, Cancer Res. 45 (1985) 5617–5624.

[25] F.J. Gonzalez, S. Kimura, D.W. Nebert, Comparison of the flanking regions and introns of the mouse 2,3,7,8-tetrachlorodibenzo-*p*-dioxin-inducible cytochrome P1-450 and P3-450 genes, J. Biol. Chem. 260 (1985) 5040–5049.

[26] I. Chung, E. Bresnick, Regulation of the constitutive expression of the human CYP1A2 gene: cis elements and their interactions with proteins, Mol. Pharmacol. 47 (1995) 677–685.

[27] M.B. Kumar, G.H. Perdew, Nuclear receptor coactivator SRC-1 interacts with the Q-rich subdomain of the AhR and modulates its transactivation potential, Gene Expr. 8 (1999) 273–286.

[28] R. Muangmoonchai, D. Smirlis, S.C. Wong, M. Edwards, I.R. Phillips, E.A. Shephard, Xenobiotic induction of cytochrome P450 2B1 (CYP2B1) is mediated by the orphan nuclear receptor constitutive androstane receptor (CAR) and requires steroid co-activator 1 (SRC-1) and the transcription factor Sp1, Biochem. J. 355 (2001) 71–78.

[29] T.V. Beischlag, S. Wang, D.W. Rose, J. Torchia, S. Reisz-Porszasz, K. Muhammad, W.E. Nelson, M.R. Probst, M.G. Rosenfeld, O. Hankinson, Recruitment of the NCoA/SRC-1/p160 family of transcriptional coactivators by the aryl hydrocarbon receptor/aryl hydrocarbon receptor nuclear translocator complex, Mol. Cell. Biol. 22 (2002) 4319–4333.

[30] J. Zhang, W. Huang, S.S. Chua, P. Wei, D.D. Moore, Modulation of acetaminophen-induced hepatotoxicity by the xenobiotic receptor CAR, Science 298 (2002) 422–424.

Distinct response to dioxin in an arylhydrocarbon receptor (AHR)-humanized mouse

Takashi Moriguchi*, Hozumi Motohashi*†, Tomonori Hosoya*‡, Osamu Nakajima*, Satoru Takahashi*, Seiichiroh Ohsako†§, Yasunobu Aoki†§, Noriko Nishimura†§, Chiharu Tohyama†§, Yoshiaki Fujii-Kuriyama*†‡, and Masayuki Yamamoto*†‡¶

*Institute of Basic Medical Sciences, Center for Tsukuba Advanced Research Alliance, and ‡Exploratory Research for Advanced Technology Environmental Response Project, University of Tsukuba, Tsukuba 305-8575, Japan; §Environmental Health Sciences Division, National Institute for Environmental Studies, Onogawa, Tsukuba 305-8506 Japan; and †Core Research for Evolutional Science and Technology, Japan Science and Technology Corporation, Kawaguchi 332-0012, Japan

Edited by Ronald M. Evans, The Salk Institute for Biological Studies, San Diego, CA, and approved March 19, 2003 (received for review December 26, 2002)

There are large inter- and intraspecies differences in susceptibility to dioxin-induced toxicities. A critical question in risk assessment of dioxin and related compounds is whether humans are sensitive or resistant to their toxicities. The diverse responses of mammals to dioxin are strongly influenced by functional polymorphisms of the arylhydrocarbon receptor (AHR). To characterize responses mediated by the human AHR (hAHR), we generated a mouse possessing hAHR instead of mouse AHR. Responses of these mice to 2,3,7,8-tetrachlorodibenzo-*p*-dioxin (TCDD) and 3-methylcholanthrene were compared with the responses of naturally sensitive (C57BL/6J) and resistant (DBA/2) mice. Mice homozygous for h*AHR* exhibited weaker induction of AHR target genes such as *cyp1a1* and *cyp1a2* than did C57BL/6J ($Ahr^{b\text{-}1/b\text{-}1}$) mice. DBA/2 ($Ahr^{d/d}$) mice were less responsive to induction of *cyp* genes than C57BL/6J mice. hAHR and DBA/2 AHR exhibit similar ligand-binding affinities and homozygous h*AHR* and $Ahr^{d/d}$ mice displayed comparable induction of AHR target genes by 3-methylcholanthrene. However, when TCDD was administered, a greatly diminished response was observed in homozygous h*AHR* mice compared with $Ahr^{d/d}$ mice, indicating that hAHR expressed in mice is functionally less responsive to TCDD than DBA/2 AHR. After maternal exposure to TCDD, homozygous h*AHR* fetuses developed embryonic hydronephrosis, but not cleft palate, whereas fetuses possessing $Ahr^{b\text{-}1}$ or Ahr^{d} developed both anomalies. These results suggest that hAHR may define the specificity of the responses to various AHR ligands. Thus, the hAHR knock-in mouse is a humanized model mouse that may better predict the biological effects of bioaccumulative environmental toxicants like TCDD in humans.

human | C57BL6/J | DBA/2 | CYP1A1

Polycyclic aromatic hydrocarbons (PAH) and halogenated aromatic hydrocarbons (HAH), including 2,3,7,8-tetrachlorodibenzo-*p*-dioxin (TCDD), benzo[*a*]pyrene, and polychlorinated biphenyls, are ubiquitous environmental toxicants whose chemical stability and lipophilicity make them highly persistent in the environment and in living organisms. These groups of chemicals cause various toxicological and biological responses, typified by teratogenesis, thymic atrophy, severe epithelial disorders, wasting syndrome, tumor promotion, and induction of xenobiotic-metabolizing enzymes in experimental animals (1, 2). The toxicities of these compounds are mediated by a conserved signaling pathway (1–4) through binding to and activation of the arylhydrocarbon receptor (AHR). AHR activation in turn mediates a transcriptional response for genes regulated by this transcription factor (5–8). Despite strong conservation of this pathway, there are wide inter- and intraspecies differences in the toxicological responses to AHR ligands (9–11). The molecular basis for these species and strain differences appears to relate to polymorphisms in AHR. Factors influencing susceptibility to the toxicity of TCDD have been studied in several animal models. There is a 10-fold difference in susceptibility between the dioxin-sensitive C57BL/6 and the resistant DBA/2 strains of mice that can be explained by polymorphic variations in the ligand-binding domain and in the C-terminal region of the AHR molecule of each strain (9, 12–14). Response to TCDD in the Long–Evans (sensitive) and Han/Wistar rats (resistant) differs by >1,000-fold due to a critical point mutation in the transactivation domain in the AHR of the Han/Wistar rat (15–17).

The effects of TCDD on humans are less well understood, although high incidences of chloracne, teratogenicity, and abortion have been associated with high blood concentrations of dioxin and related compounds in residents of regions where industrial accidents or extensive use of dioxin-containing defoliants have resulted in human exposures (3). Increased levels of dioxin in the body have been reported recently to be associated with abnormal sex ratio of newborns nearly 25 years after the accident in Seveso, Italy (18). Because the AHR primarily mediates the pleiotropic manifestations of dioxin exposure, characterization of the structural and functional properties of the human AHR (hAHR) is critical for understanding the types and magnitudes of human responses to various PAH/HAHs.

To date, *in vitro* characterization of the hAHR has provided ambiguous insights into human sensitivity to dioxin. The dissociation constant (K_d) of hAHR for TCDD was comparable to that of TCDD-resistant DBA/2 AHR (9, 19), suggesting that humans might be resistant to TCDD. By contrast, high homology of the human receptor to the AHR of the guinea pig, which is the most sensitive animal to TCDD, suggests a high responsiveness of humans to the toxin (20). Ligand specificity of hAHR was also examined and compared with those of zebrafish and rainbow trout AHRs using polychlorinated dibenzo-*p*-dioxin, dibenzofuran, and biphenyl congeners as test ligands. These studies revealed that mono-ortho polychlorinated biphenyls activated hAHR but were not very effective in activating either zebrafish or rainbow trout AHRs (21).

Assessment of human responses *in vivo* to unintended exposures to various PAH/HAHs has been hampered by limited exposure assessments and toxicological follow-up. Observational studies after intentional exposures have not been and should not be conducted. To gain stronger insight into the hazards to human health posed by compounds interacting with the hAHR *in vivo*, we generated a mouse model that harbors the hAHR cDNA instead of the mouse *AhR* gene. This mouse may reveal a humanized susceptibility to chemical toxicities. In response to challenges with 3-methylcholanthrene (3-MC) and TCDD, two prototypical AHR ligands, the hAHR knock-in

This paper was submitted directly (Track II) to the PNAS office.

Abbreviations: AHR, aryl hydrocarbon receptor; hAHR, human AHR; h*AHR*, human AHR knock-in allele; Ahr^{d}, DBA/2 *Ahr* allele; $Ahr^{b\text{-}1}$, C57BL/6 *Ahr* allele; TCDD, 2,3,7,8-tetrachlorodibenzo-*p*-dioxin; 3-MC, 3-methylcholanthrene; PAH, polycyclic aromatic hydrocarbons; HAH, halogenated aromatic hydrocarbons; ES, embryonic stem; GD, gestation day.

¶To whom correspondence should be addressed. E-mail: masi@tara.tsukuba.ac.jp.

www.pnas.org/cgi/doi/10.1073/pnas.1037886100